TRANSMISSION MEASUREMENTS USING A NEW FAR-INFRARED SET-UP

By

Katarin Alinta Baskin

B. Sc. (Physics) St. Francis Xavier University

A THESIS SUBMITTED IN PARTIAL FULFILLMENT OF

THE REQUIREMENTS FOR THE DEGREE OF

MASTER OF SCIENCE

in

THE FACULTY OF MATHEMATICS AND SCIENCE

DEPARTMENT OF PHYSICS

We accept this thesis as conforming

to the required standard

.....

.....

.....

.....

.....

BROCK UNIVERSITY

August 1996

In presenting this thesis in partial fulfilment of the requirements for an advanced degree at Brock University, I agree that the Library shall make it freely available for reference and study. I further agree that permission for extensive copying of this thesis for scholarly purposes may be granted by the head of my department or by his or her representatives. It is understood that copying or publication of this thesis for financial gain shall not be allowed without my written permission.

_____

Department of Physics
Brock University
500 Glenridge Avenue
St. Catharines, Ontario
Canada L2S 3A1

Date:

_____

Abstract

A system comprised of a Martin-Puplett type polarizing interferometer and a Helium-3 cryostat was developed to study the transmission of materials in the very-far-infrared region of the spectrum. This region is of significant interest due to the low-energy excitations which many materials exhibit. The experimental transmission spectrum contains information concerning the optical properties of the material. The set-up of this system is described in detail along with the adaptations and improvements which have been made to the system to ensure the best results.

Transmission experiments carried out with this new set-up for two different varieties of materials: superconducting thin films of lead and biological proteins, are discussed.

Several thin films of lead deposited on fused silica quartz substrates were studied. From the ratio of the transmission in the superconducting state to that in the normal state the superconducting energy gap was determined to be approximately 25 cm^{-1} which corresponds to $2\Delta/k_BT_C \sim 5$ in agreement with literature data. Furthermore, in agreement with theoretical predictions, the maximum in the transmission ratio was observed to increase as the film thickness was increased. These results provide verification of the system's ability to accurately measure the optical properties of thin low-T_C superconducting films.

Transmission measurements were carried out on double deionized water, and a variety of different concentrations by weight of the globular protein, Bovine Serum Albumin, in the sol, gel and crystalline forms. The results of the water study agree well with literature values and thus further illustrate the reproducibility of the system. The results of the protein experiments, although preliminary, indicate that as the concentration increases

the samples become more transparent. Some weak structure in the frequency dependent absorption coefficient, which is more prominent in crystalline samples, may be due to low frequency vibrations of the protein molecules.

Table of Contents

List of Tables

List of Figures

Acknowledgements

I would like to take this opportunity to thank all of the people who have contributed to the lab in the past two years. I am grateful to my supervisor, Dr. Maureen Reedyk, for providing me with a very challenging project and the opportunity for developing independent research skills. She has allowed me to explore materials of my own interest for which I thank her. Her guidance and support, understanding and patience have been greatly appreciated. I would also, at this time, like to express my appreciation for the opportunities to attend conferences and meet with visitors. To the other members of my committee, I am also grateful. Dr. Razavi has taught me numerous things concerning sample preparation, and Dr. Mitrović has always expressed interest in my project. Both have participated in my project and continued to show interest and provide stimulating discussions.

A great deal of fine tuning of the equipment was completed through collaboration with Marko Scholze, and from this I have learned the true meaning of collaboration. To the other members of our group, Judy Baranowski, Chris Braun, Halima Hawesa, Thomas Kieliba, and Mylo Hildebrand, good luck and I thank you for all of the contributions you have made to the lab.

I have also benefited from the discussions I have had with Dr. Pink and Dr. Rowell. I am also grateful to Dr. Nicol for providing me with the Fortran program described in chapter 4, as well as for interesting discussions throughout the past year. I also thank the biology department for providing the BSA sample and the machine shop and the electronics shop for their fine craftsmanship and great sense of humor. To Alice, who always knew where to find the late passes, Frank for ordering the helium and other

supplies and to John for his constant supply of liquid nitrogen, I thank you.

Finally, I extend a warm thank you to my office mates, Stephanie Recker and Jim Murdoch, for their patience and understanding, to my friends, Stef, Judy, Ron, Launy, Bill and Marko for keeping my spirits high when times were tough, to the members of the City of Thorold Pipe Band for their great wit, and lastly, to my family for their support and encouragement. To all of you, I extend a heartfelt thank you for everything.

Chapter 1

Introduction

Since ancient times, mankind has been intrigued by luminescence and there have been many who have reported on how light interacts with various materials. However, if one must assign a date to 'modern' studies of spectroscopy, then 1888 would be appropriate. It was in that year, E. Wiedemann reported that quinine, esculin and many other 'dyestuffs' when absorbed in gelatin, phosphoreced more strongly at -80°C than at room temperature. After this, Dewar, in 1894, reported that many bodies when cooled to temperatures between -180°C and -200°C, after stimulation by light, become remarkably phosphorescent, not only increasing in intensity, but also in duration. This was the beginning of low temperature spectroscopy.[1]

Far-infrared studies were begun at the turn of the last century, and a well known pioneer of this field was H. Rubens. In the early days, monochromators employing a grating as dispersion element were used for obtaining spectral data. This type of grating spectrometer was the primary tool for studying the spectral range of 50μm to 1000μm until the introduction of interferometers using the principles of Fourier transform spectroscopy. By the 1960's, commercially available spectrometers accelerated developments in the field. Further developments of commercially available low temperature detectors and cryostats have also benefited this field. Using these products, researchers have been able to reach new limits not only in temperature, but also in frequency resulting in an ability to probe the very low energy excitations of materials by carrying out experiments in the very-far-infrared region.[2]

The subject of this thesis is the development of a far-infrared system capable of measuring the transmission of materials at temperatures as low as 0.5 K and frequencies as low as a few wavenumbers. Chapters two and three deal with aspects of the instrumentation and underlying theory respectively, while chapters four and five discuss the results of transmission measurements carried out on superconducting thin films and biological samples, respectively.

Chapter two focuses on the equipment which has been purchased or constructed in-house and the way in which it has been developed to enable transmission measurements to be carried out. A detailed description is provided of each of the major components of the system and how they function in order to give a 'signal' which can be measured. Chapter three then explains how this 'signal' is transformed into a meaningful optical quantity. The basics of obtaining optical properties from Maxwell's equations and extracting them from the measured transmittance are discussed.

The chapters which deal with the experimentally obtained data are chapters four and five. Chapter four is concerned with measurements of thin superconducting films made from the evaporation of lead onto fused silica quartz substrates. A brief introduction to superconductivity and far-infrared transmission of superconductors is given, followed by a discussion of the data obtained. From comparisons with the literature, it is found that there is good agreement and thus the conclusion can be made that the system is indeed working properly.

Chapter five focuses on transmission measurements of various 'liquids'. It begins with a short theory section to explain how meaningful results are obtained. This is followed by a detailed explanation of how the transmission optical cells were created and how the measurements were carried out. As a check of the system and the experimental procedure, the transmission of liquid water was measured and analyzed. Finding this result in good agreement with the literature, further study of biological materials, a

long standing interest of the author, was initiated. The system chosen was the globular protein, Bovine Serum Albumin, which could be prepared in a sol, gel, or crystalline form.

Although transmission measurements may be considered 'simple' and to a certain extent 'uninteresting' by the uninitiated, the author feels that this thesis illustrates not only that these measurements are worthwhile and nontrivial, especially in terms of sample preparation, but that for the biological samples, this may be the only way in which to gain some understanding of the very low energy vibrations that these samples possess.

Chapter 2

Instrumentation

2.1 General Overview

The far-infrared system that has been developed is composed of four main items: a Martin-Puplett-type polarizing interferometer, connecting lightpipes, a Helium-3 cryostat, and the controlling electronics. A block diagram of the system is shown in figure 2.1. It illustrates the different components of the system and their lines of communication.

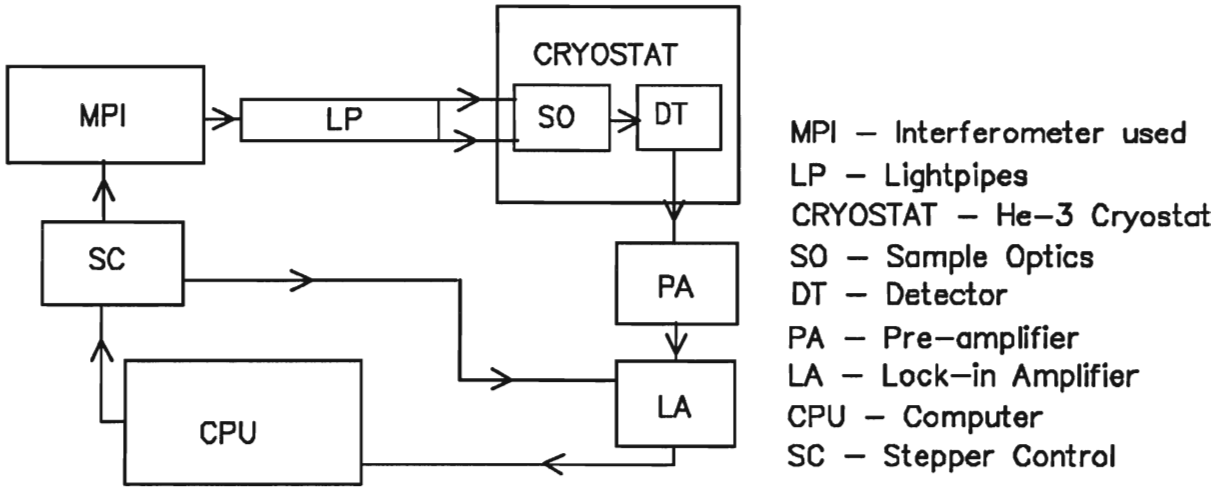

Figure 2.1: **Components comprising the far-infrared system with their lines of communication.**

2.2 System Specifics

2.2.1 Martin-Puplett Interferometer

One of the key components of a far-infrared system is the spectrometer which is used to provide the radiation to examine the sample. The type of spectrometer used for the experiments discussed herein was a Martin-Puplett-type polarizing interferometer (MPI) manufactured by Sciencetech Inc. This design was first introduced by Martin and Puplett in 1969, and is based on the standard Michelson with a few improvements.[3] These improvements include a polarizing wire grid beamsplitter and rooftop mirrors, where the angle between the two reflecting surfaces is 90°, to replace the standard flat mirrors found in the Michelson. The layout of the components can be seen in figure 2.2.

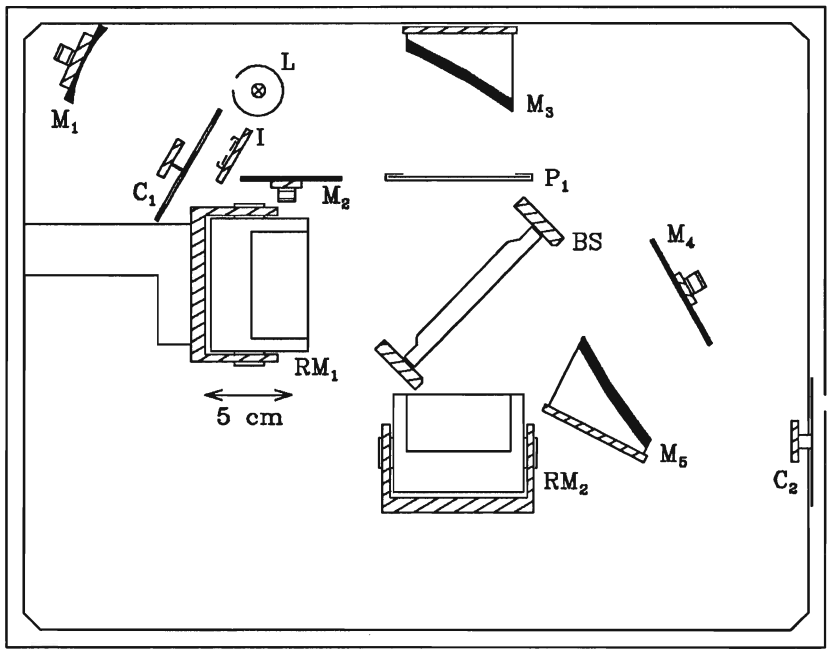

Figure 2.2: **A schematic of the MPI.**[4]

The main feature of this MPI is the polarizing beamsplitter. It is a holographic wire

grid etched onto a mylar substrate. This grid will reflect incident light whose component is parallel to its holographic wires, and transmit the incident light whose component is perpendicular to its holographic wires.

The MPI works in the following manner: light from a mercury-xenon lamp is reflected from a series of mirrors and eventually passes through the first polarizer, P_1, which has been oriented such that the lines of the wire grid horizontally plane polarize the light. The light then passes through the beamsplitter, BS, which is also a polarizer. Its lines form an angle of 45° with respect to the lines of P_1. Therefore, the beamsplitter separates the incoming light into two equal parts, one component which is reflected to the moveable rooftop mirror, RM_1, and the second which is transmitted to the stationary rooftop mirror, RM_2. The planes of polarization of each of these beams are then rotated by 90° via reflection from the rooftop mirrors.[5] It is then clear that the light from RM_1 will be transmitted through BS and the light from RM_2 will be reflected by BS resulting in a recombination of the two beams. Due to the movement of RM_1, a phase difference between the two beams occurs resulting in the recombined beam being elliptically polarized. The light is then passed through the output polarizing chopper, C_2, and emerges plane polarized. It should be noted that if RM_1 and RM_2 are at equal distances from BS, then the polarization of the recombined beam will be the same as that of the initial incident radiation.

As reported by [3] the efficiency of the BS is approximately 100% in the range of 0 to $1/2d\ cm^{-1}$, where d is the grid constant and in our case is equal to $4 \times 10^{-4}\ cm$. This implies a range from 0 to 1250 cm^{-1}. Thus, the MPI, in principle, could be used over a wider far-infrared spectral range than the standard Michelson, as has been reported by [6].

Another important feature of the MPI is the absence (at least in principle) of a dc offset of the interferogram. This results from modulating the polarization of the output

beam. This is particularly advantageous because it minimizes errors arising from the Fourier transformation.[7] The travel distance of RM_1 is 5 cm, 1 cm to the left of the zero path and 4 cm to the right. This gives a maximum optical path difference , X, of 8 cm. As stated by [8], the resolution for a two beam interferometer is $1/2X$, and therefore, the theoretical limit of resolution for a symmetric interferogram is 0.25 cm^{-1} and for an asymmetric interferogram is 0.06 cm^{-1}.

2.2.2 Lightpipes

The lightpipes are of a unique design and have been especially constructed for this particular set-up. As can be seen in figure 2.3, they are in the shape of a "Y" with the base of the "Y" attached to the MPI via a flange with a vacuum seal. The two arms of the "Y" are attached to the windows of the cryostat with similar fixtures. The lightpipes are constructed of thin, highly polished brass tubing, with a rotatable stainless steel mirror (or 'flip' mirror) at the intersection. The light enters the lightpipes from the MPI, and depending on the orientation of the flip mirror, either travels through the reference path or the sample path. There are two shutters, one located on each arm. These are necessary to ensure that any radiation which leaks past the flip mirror and travels along the arm not in use does not make its way into the cryostat, giving an incorrect result for the arm being measured. During a measurement, the shutter on one arm is open while that on the other is closed. The flip mirror angle is adjusted in order to maximize the signal. After both positions of the flip mirror have been adjusted, ie. one position for each arm, the adjustment screws are locked into place with locking nuts. The flip mirror can then be rotated between these two positions. The lightpipes and the MPI are both evacuated during an experiment and use the same vacuum system.

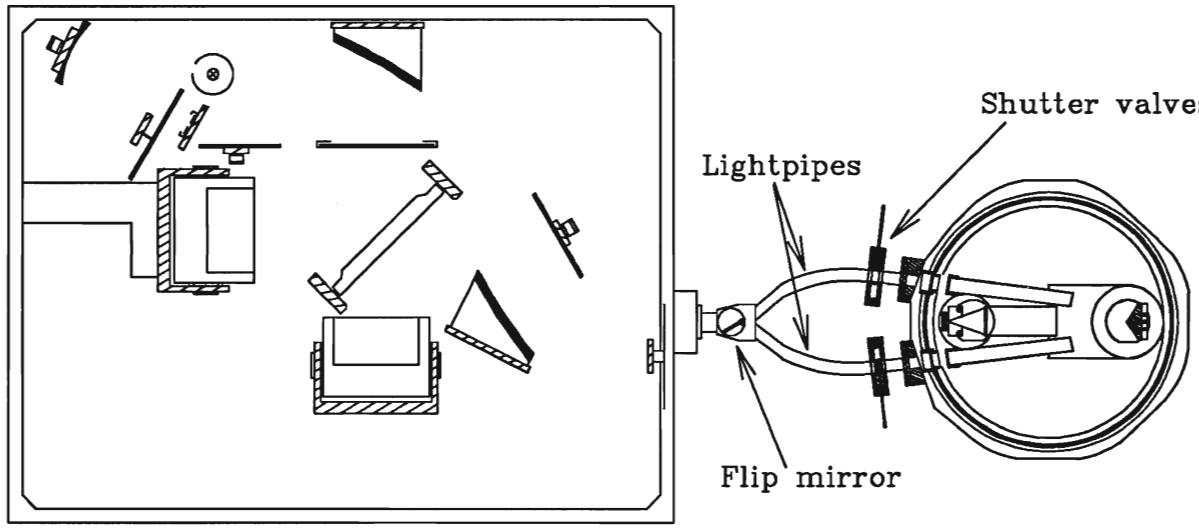

Figure 2.3: **The lightpipes, shutter valves and 'flip' mirror of the far-infrared system.[4]**

2.2.3 Helium-3 Cryostat

The basic function of a cryostat is as a sample holder that will provide refrigeration to cool the sample. It requires a vacuum shroud to thermally insulate the sample, and an optical path for observation and excitation with incident radiation.[9] The cryostat used for the measurements discussed herein has been purchased from IRLabs Inc. It has been designed so that both the sample and the detector are located inside the cryostat and are capable of reaching Helium-3 temperatures. This cryostat design is unique, not only because of the low temperatures that it is able to reach, but also because of the two paths for incident light: one specifically for the reference and the other for the sample. This reduces the number of moving parts inside the cryostat and, as a result improves the thermal contact between the sample and the cold stage. From figure 2.4, one can see how items have been arranged within the cryostat so that light of near normal incidence can be reflected from the sample into the detector.

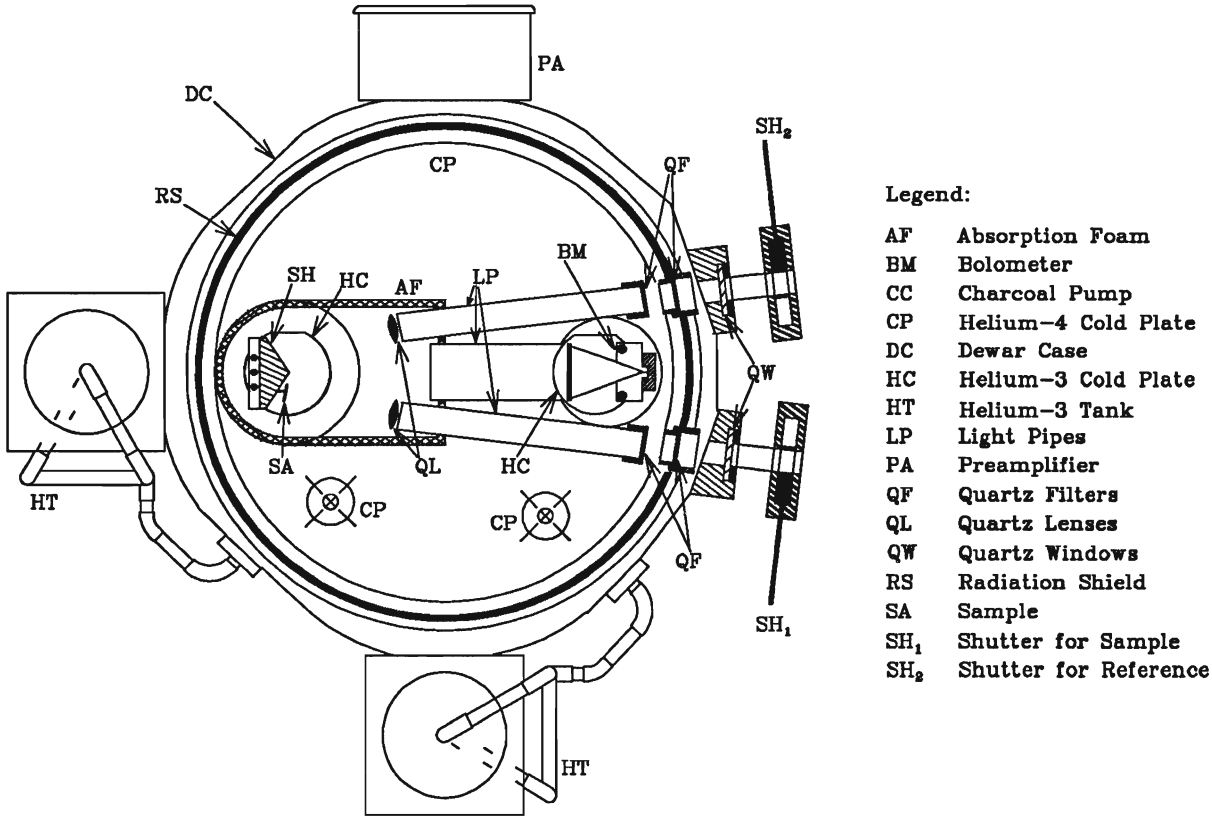

Figure 2.4: **The components of the cryostat, as seen from looking down, into the cryostat.**[4]

Detectors

There have been two different detectors used with this particular cryostat, one specifically designed for the low wavenumber region of the spectrum ($3 - 40\ cm^{-1}$), and one for a higher region ($30 - 150\ cm^{-1}$). The detectors, or as they are properly named, resistance bolometers, have an electrical resistivity which depends very strongly on temperature.[10] The light, incident on the detector, is absorbed, resulting in a temperature change of the detector. This change in temperature corresponds to a change in the resistance of the absorbing element which is in this particular case, a doped silicon chip. This element has been thermally bonded to a suitably blackened 5.0 mm diameter sapphire absorber. It has been mounted in a cylindrical cavity, and the absorbing layer was selected for maximum absorbence. The detectors are mounted in a side looking configuration in conjunction with a gold plated Winston cone collector and a far-infrared (cut-on) type filter. The filter for the low temperature detector has a 285 micron cut-on while for the higher temperature detector, a 40 micron cut-on is used. The Winston cone entrance aperture is 16 mm, and it has a focal ratio of 5.0. The exit aperture is 4 mm. [11, 12]

The process of cooling the cryostat begins with a liquid nitrogen pre-cool which is then expelled and replaced with liquid helium. The cryostat reaches helium-3 temperatures (0.3K) through the use of two helium-3 refrigeration devices. As can be seen in figure 2.5, each refrigerator consists of two reservoirs, P and E, connected by a tube and two heat switches $S1$ and $S2$. The process begins with the system coming to thermal equilibrium with the heat reservoir, this being the helium-4 bath. Both heat switches ($S1$ and $S2$) on both refrigerators begin in the closed position, or rather in the heat conducting position. This brings both the sample and the bolometer stage to 4.2 K, the temperature of liquid helium-4. After all of the helium-3 gas has been adsorbed onto the charcoal in chamber P, the helium-4 bath is pumped, reducing its temperature well

below the critical temperature of helium-3, 3.3 K. At the start of the pumping process, switch $S2$ for the charcoal pump is opened and the heater, H, is energized to bring the cryopump to 25K, causing the charcoal to expel the helium-3. The gas pressure of the helium-3 will rise and when it exceeds the vapor pressure at the temperature of the helium-4 bath, condensation in the helium-3 chamber, E, occurs, with a latent heat of condensation, L_1, and enthalpy change of the gas, ΔH, conducted to the helium-4 bath by the first switch, $S1$. The 'heat load' on the helium-4 bath is thus $Q1 = L1 + \Delta H$. The second process in the helium-3 cooling is the evaporation. With $S1$ open, and $S2$ closed, and the heater, H, turned off, the cooling charcoal will begin to adsorb the helium-3 gas, thus lowering the pressure above the helium-3 bath. The temperature of the helium-3 chamber will eventually stabilize at approximately 0.3 K. It will stay at this temperature until all of the remaining helium-3 has been evaporated or until the adsorbent becomes saturated. This system can be recycled during an experiment and is always recycled after the experiment is over.[12]

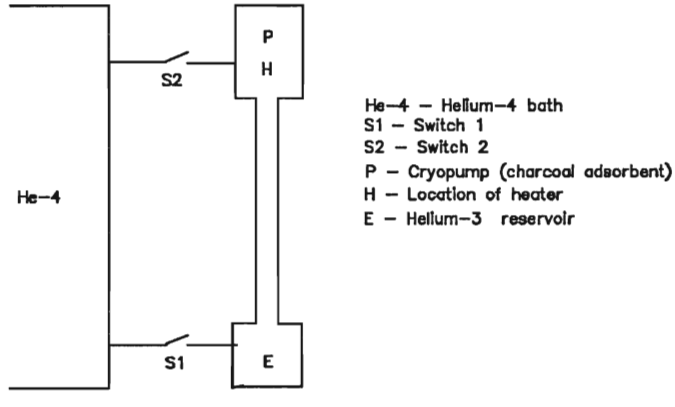

Figure 2.5: **Components of the charcoal pump Helium-3 system.[12]**

The cryostat is also equipped with a preamplifier which amplifies the signal by either a gain of 200 or 1000.

Lenses

Since the beam exiting the incident lightpipe is somewhat divergent, resulting in the light being poorly focused on the sample holder (which for the experiments reported in this thesis was used to hold a gold plated stainless steel mirror) it was decided that a fused silica quartz lens system would be beneficial to focus the beam onto the mirror. Based on the calculation given in [13], space restrictions of the sample chamber, and the index of refraction of fused silica in the far-infrared region reported in [14], lenses which were 12.7mm in diameter, with a focal length of 51 mm and a center thickness of 2.0 mm were purchased. A consequence of using the lightpipes and lenses is that a diffraction pattern occurs and then is focused onto the mirror.

Absorption Foam

Since the sample chamber was constructed of aluminum and brass and the light, as a result of the diffraction, is not focussed to a perfect spot, a large background signal was present, and thus extracting small changes in the signal coming from the sample was rather difficult. Therefore, absorption foam was added to the sample chamber to aid in the reduction of the background signal. The foam was either glued with a small amount of GE varnish, or just securely wedged into place. It was found that the foam essentially eliminated the background signal and light leaks.

2.2.4 Controlling Program and Electronics

The preamplified signal is measured with a lock-in amplifier. A lock-in is used to detect small ac signals, and it is possible to obtain a signal even when the noise is larger than the signal. A signal which comes from the chopper control is used as a reference, and the phase between this signal and the detector signal can be minimized through the lock-in

control panel. The initial computer program which was used to control most aspects of the experiment is written in Quick Basic and was provided with the interferometer. The program was adapted for this particular system in a number of different ways. First, interfacing to the lock-in amplifier was completed through the use of an RS232 cable. A simple graphics routine was also written so that the interferogram could be viewed in real time. The program; listed in Appendix A, controls the stepping motor, chopper, and lock-in as well as collects, saves and graphs the data. Currently, a program written in C++ by Thomas Kieliba is used. A listing of this program can be found in [15]. The flip mirror and shutters located on the lightpipes are still changed through manual operation.

Chapter 3

Theory

3.1 Introduction

The focus of chapter 2 was on the way in which the different components of the far-infrared system work together with the result that after somehow interacting with the sample, light incident on a detector is converted to a meaningful signal. There are two aspects of this process which require a more thorough mathematical treatment. These will be dealt with in this chapter. In section 3.2, an explanation is given of how one is able to obtain a plot of intensity as a function of frequency by observing the changes in the signal intensity as the roofmirror, RM_1, moves. This is followed by sections 3.3 and 3.4 which discuss how it is possible to extract from this plot of intensity versus frequency, the optical properties of the sample.

3.2 Fourier Transform Spectroscopy

The technique of Fourier transform spectroscopy provides a way to transform a measurement of the intensity of light as a function of path difference into a power spectrum of intensity versus frequency. It is a standard technique which has been utilized for many years. The discussion that follows is based on that presented in reference [2]. For further details, references [16, 8, 17] and [18] can be consulted.

As a starting point for understanding this technique, one is reminded of the discussion in chapter 2 concerning the operation of the polarizing interferometer. The light after

having travelled to the beamsplitter, BS, is divided into two beams. Beam I is reflected to RM_1, while beam II is transmitted to RM_2. Recall, RM_1 is the only mirror which is moveable. After the beams are reflected from their respective rooftop mirrors, they recombine constructively or destructively. The plot of the intensity of this recombination of the two beams as a function of the optical path difference is called an interferogram. The position of the mirror at which the maximum of the interferogram occurs is referred to as the zero path position since the distance between each rooftop mirror and the beamsplitter is equal. It is here that the most constructive interference takes place. If the interferogram is then Fourier transformed, a plot of intensity as a function of frequency is obtained where the frequency is measured in wavenumbers (cm^{-1}). This result is referred to as a power spectrum. The rooftop mirror, RM_1, is controlled by a stepper motor, and so the experiment is carried out in a 'step and integrate' fashion. For each position, a wait time is defined so that enough averaging can be done to reduce noise and record the interferogram. Fourier transform spectroscopy is a preferred technique because of it's high signal-to-noise ratio.

As a first approximation, if one considers the light source to be monochromatic, having a frequency of ν_0, with a displacement of RM_1 of $x/2$, where $x = 0$ at the zero path, then the superposition of beams I and II can be expressed as

$$g(x) = 4S\cos^2(\pi\nu_0 x) = 2S(1 + \cos[2\pi\nu_0 x]) \tag{3.1}$$

where $\sqrt{S}$ is the fractional amplitude of each of the recombined beams.

However, the light from the source is not monochromatic. It consists of a continuous spectrum of frequencies, $0 \leq \nu_0 \leq \infty$, and thus S becomes a function of frequency. The function $g(x)$ then becomes an integral where the limits are $0 \leq \nu_0 \leq \infty$:

$$g(x) = 2\int_0^\infty S(\nu)(1 + \cos[2\pi\nu x])d\nu.$$

This can be written as:

$$g(x) = \int_0^\infty 2S(\nu)d\nu + \int_0^\infty 2S(\nu)\cos[2\pi\nu x])d\nu. \tag{3.2}$$

At the zero path position where $x = 0$ this equation simplifies to:

$$g(0) = 2\int_0^\infty 2S(\nu)d\nu. \tag{3.3}$$

From equations 3.2 and 3.3, it is possible to write down what is known as the interferogram function:

$$s(x) = g(x) - \frac{1}{2}g(0)$$

$$s(x) = \int_0^\infty 2S(\nu)\cos[2\pi\nu x]d\nu. \tag{3.4}$$

The interferogram function gives the intensity, s, as a function of distance, x. Now, if one applies the cosine Fourier transform theorem to equation 3.4, one obtains the following pair of Fourier transforms:

$$s(x) = \int_{-\infty}^\infty S(\nu)\cos[2\pi\nu x]d\nu, \tag{3.5}$$

$$S(\nu) = \int_{-\infty}^\infty s(x)\cos[2\pi\nu x]dx. \tag{3.6}$$

As can be seen from the limits of the integration, the interferogram is infinitely long. In an experimental environment, this is impossible to achieve since one is restricted by the finite travel distance of the moveable mirror, RM_1. If this travel distance is referred to as

D then the corresponding optical path difference is $L = 2D$. Thus, if the interferogram function is multipied by a box function,

$$p(x) = \begin{cases} 1 & \text{for } -L \leq x \leq L \\ 0 & \text{otherwise.} \end{cases} \tag{3.7}$$

the limits of x can remain. Therefore the integral in equation 3.6 becomes

$$S_{box}(\nu) = \int_{-\infty}^{\infty} s(x)p(x)\cos[2\pi\nu x]dx. \tag{3.8}$$

This expression for $S_{box}(\nu)$ can also be expressed using the convolution theorem which states that the Fourier transform of the product of two functions is the convolution of the Fourier transforms of the individual functions. Therefore, $S_{box}(\nu)$ becomes

$$S_{box}(\nu) = \int_{-\infty}^{\infty} S(\tau)P(\nu - \tau)d\tau. \tag{3.9}$$

Here $S(\tau)$ is

$$S(\tau) = \int_{-\infty}^{\infty} s(x)\cos[2\pi\tau x]dx, \tag{3.10}$$

while $P(\tau)$ is given by:

$$P(\tau) = \int_{-\infty}^{\infty} p(x)\cos[2\pi\tau x]dx. \tag{3.11}$$

With the limits given in equation 3.7, one obtains:

$$P(\tau) = 2L\frac{\sin[2\pi\tau L]}{[2\pi\tau L]}. \tag{3.12}$$

Because the interferogram is of a finite length, the abrupt termination of the interferogram at the limits of L and $-L$ results in a possible distortion of the spectrum to be analyzed. One must therefore be careful with the 'sidebands' that result since they can interfere with

the location and intensity of the real peaks and in so doing, falsify the spectrum obtained. Fortunately, a technique for suppressing these sidebands, referred to as apodization, can used. This is achieved by replacing $p(x)$ by a function other than the previously mentioned box function. The simplest which can be used is the triangular function:

$$h(x) = \begin{cases} 1 - \left|\frac{x}{L}\right| & \text{for } -L \leq x \leq L \\ 0 & \text{otherwise.} \end{cases} \tag{3.13}$$

The fact that the data is sampled discretely requires that the integral must be replaced by a summation over the number of data points taken, N. With an optical path difference between points of Δx, $S(\nu)$ can be written as:

$$S(\nu) = \sum_{n=0}^{N} s(n\Delta x)p(n\Delta x)\cos[2\pi\nu n\Delta x]\ \Delta x. \tag{3.14}$$

From the optical path difference interval, Δx, it is possible to determine the cutoff frequency, or rather the bandwidth of the spectrum using:

$$\nu_{max} = \frac{1}{2\Delta x}. \tag{3.15}$$

The resolution, $\Delta\nu$, is determined by the total number of data points, N. Essentially, if one uses a triangularly apodized interferogram then the resolution is simply proportional to the inverse of the maximum optical path difference, L:

$$\Delta\nu = \frac{1}{2L}. \tag{3.16}$$

As was stated above, the maximum of the interferogram function occurs at the zero path position, where $x = 0$. In an ideal situation, this point would be sampled, however, this usually does not occur. When the zero path is not sampled, all the data points are

displaced which gives rise to a phase error $\varphi(\nu)$. This will cause the interferogram to be asymmetric with respect to the zero path. In order to correct this phase error, the complete Fourier transform must be used. From the unapodized interferogram function, one obtains

$$s_1(x) = \int_{-\infty}^{\infty} S(\nu) e^{-i2\pi\nu x} d\nu. \tag{3.17}$$

If the phase error is then included, $s_1(x)$ becomes

$$s_1(x) = \int_{-\infty}^{\infty} S(\nu) e^{-i\varphi(\nu)} e^{-i2\pi\nu x} d\nu. \tag{3.18}$$

The Fourier transform of $S(\nu)e^{-i\varphi(\nu)}$ is $s_1(x)$ and therefore

$$S(\nu)e^{-i\varphi(\nu)} = \int_{-\infty}^{\infty} s_1(x) e^{i2\pi\nu x} dx. \tag{3.19}$$

This expression can then be separated into real and imaginary parts yielding

$$S(\nu)e^{-i\varphi(\nu)} = P(\nu) + iQ(\nu). \tag{3.20}$$

Finally the phase can be calculated:

$$\varphi(\nu) = -\arctan \frac{Q(\nu)}{P(\nu)}. \tag{3.21}$$

3.3 The Optical Properties of Solids

The optical properties of solids can be extracted from a set of equations which describe how light interacts with different media. Although an elementary discussion can be found in a variety of different texts concerning solid state physics, such as [19], and a more detailed description can be found in [20], a summary shall be given of the more important points in this section, while the theory of transmittance will be discussed in the following section.

In order to examine the optical properties of solids one begins from Maxwell's equations, which, given in Gaussian units, are:

$$\nabla \times \mathbf{H} - \frac{1}{c}\dot{\mathbf{D}} = \frac{4\pi}{c}\mathbf{J}, \tag{3.22}$$

$$\nabla \times \mathbf{E} + \frac{1}{c}\dot{\mathbf{B}} = 0, \tag{3.23}$$

$$\nabla \cdot \mathbf{D} = 4\pi\rho, \tag{3.24}$$

$$\nabla \cdot \mathbf{B} = 0, \tag{3.25}$$

where $\mathbf{H}$ is the magnetic vector, $\mathbf{D}$ is the electric displacement, $\mathbf{J}$ is the electric current density, $\mathbf{E}$ and $\mathbf{B}$ are the electric and magnetic field vectors and ρ the electric charge density.

Since the electromagnetic field is interacting with a material, namely the sample, the material equations which describe this interaction must be incorporated into the Maxwell equations. For isotropic materials, these tensor equations reduce to:

$$\mathbf{J} = \sigma\mathbf{E}, \tag{3.26}$$

$$\mathbf{D} = \epsilon\mathbf{E}, \tag{3.27}$$

$$\mathbf{B} = \mu\mathbf{H}. \tag{3.28}$$

The constants, known as material constants are the specific conductivity, σ, and the dielectric and magnetic permittivity, ϵ and μ respectively. From here, Maxwell's equations can be written as

$$\nabla \times \mathbf{H} - \frac{\epsilon}{c}\dot{\mathbf{E}} = \frac{4\pi}{c}\sigma\mathbf{E}, \tag{3.29}$$

$$\nabla \times \mathbf{E} + \frac{\mu}{c}\dot{\mathbf{H}} = 0, \tag{3.30}$$

$$\nabla \cdot \mathbf{E} = \frac{4\pi}{\epsilon}\rho, \tag{3.31}$$

$$\nabla \cdot \mathbf{H} = 0. \tag{3.32}$$

If one assumes that ρ can be divided into a part which is due to the polarization $\mathbf{P}$ of the electronic charges caused by the electric field and a part which is due to external charges then,

$$\rho = -\nabla \cdot \mathbf{P} + \rho^{ext}. \tag{3.33}$$

If one assumes an isotropic medium so that ϵ is spatially invariant, and that no external charges are present, equation 3.31 can be written as:

$$\nabla \cdot \mathbf{E} = 0. \tag{3.34}$$

From here, elimination of $\mathbf{H}$ in equation 3.29 can be performed by use of the vector identity

$$\nabla \times (\nabla \times \mathbf{E}) = \nabla(\nabla \cdot \mathbf{E}) - \nabla^2\mathbf{E}. \tag{3.35}$$

Combining this with equation 3.34 leads to the conclusion that $\mathbf{E}$ must satisfy the wave equation

$$\nabla^2\mathbf{E} = \frac{\mu\epsilon}{c^2}\ddot{\mathbf{E}} + \frac{4\pi\mu\sigma}{c^2}\dot{\mathbf{E}}. \tag{3.36}$$

A solution for the wave equation is

$$\mathbf{E} = \mathbf{E}_0 e^{i(\mathbf{q}\cdot\mathbf{r}-\omega t)}. \tag{3.37}$$

By substituting this solution into the wave equation, one obtains:

$$q^2 = \mu\frac{\omega^2}{c^2}(\epsilon + i\frac{4\pi\sigma}{\omega}). \tag{3.38}$$

Using the standard definition for the absolute refractive index $\hat{n}$ of a medium, $\hat{n} = c/v$, and the fact that velocity of an electromagnetic wave in a medium is given by, $v = \omega/q$, one obtains the complex refractive index:

$$\hat{n} = \sqrt{\epsilon + i\frac{4\pi\sigma}{\omega}}. \tag{3.39}$$

The complex refractive index, $\hat{n}$, is also written as:

$$\hat{n} = n + ik \tag{3.40}$$

where k is known as the extinction coefficient or more often as the absorption coefficient for transmittance measurements.

The complex dielectric function and conductivity can then be defined as:

$$\hat{\epsilon} = \epsilon_1 + i\epsilon_2, \tag{3.41}$$

$$\hat{\epsilon} = \frac{\hat{n}^2}{\mu}, \tag{3.42}$$

$$\hat{\sigma} = \sigma_1 + i\sigma_2, \tag{3.43}$$

where $\epsilon \equiv \epsilon_1$ and $\sigma \equiv \sigma_1$.

Finally, the real and imaginary parts of the dielectric function are given by:

$$\epsilon_1 = \frac{n^2 - k^2}{\mu} \tag{3.44}$$

and

$$\epsilon_2 = \frac{2nk}{\mu}, \tag{3.45}$$

while the real and imaginary parts of the optical conductivity, assuming the magnetic permittivity is one, are given by:

$$\sigma_1 = \frac{\epsilon_2 \omega}{4\pi} \tag{3.46}$$

and

$$\sigma_2 = \frac{\omega(1 - \epsilon_1)}{4\pi}. \tag{3.47}$$

3.4 Theory of Transmittance

While the material properties, $\hat{\sigma}$, $\hat{\epsilon}$, and $\hat{n}$ are the desired result, experimentally a quantity called the transmittance is measured. If one assumes that an electromagnetic wave, $\mathbf{E}$, incident on an interface between two media, is plane polarized, $\mathbf{E}$ can be written as:

$$\mathbf{E} = \mathbf{E}_0 \cos(\mathbf{q} \cdot \mathbf{r} - \omega t). \tag{3.48}$$

The reflected wave is written as:

$$\mathbf{E}_R = \mathbf{E}_{0R} \cos(\mathbf{q_R} \cdot \mathbf{r} - \omega_R t + \epsilon_R), \tag{3.49}$$

while the transmitted wave as:

$$\mathbf{E}_T = \mathbf{E}_{0T} \cos(\mathbf{q_T} \cdot \mathbf{r} - \omega_T t + \epsilon_T), \tag{3.50}$$

where ϵ_R and ϵ_T are phase constants relative to $\mathbf{E}_{0R}$ and $\mathbf{E}_{0T}$ respectively. The laws of electromagnetism state that the tangential component of the electric field must be continuous across a boundary. This implies that the tangential component of the electric field which is incident, when added to the reflected tangential component must equal the tangential component which is transmitted. If one takes a unit vector, $\hat{u}$, which is normal to the surface, one must have:

$$\hat{u} \times \mathbf{E}_I + \hat{u} \times \mathbf{E}_R = \hat{u} \times \mathbf{E}_T \tag{3.51}$$

where $\mathbf{E}_I$ is the incident electric field. This equation must be satisfied for any moment in time, and any point along the boundary. This leads to the law of reflection, see [18]:

$$\theta_I = \theta_R \tag{3.52}$$

and to Snell's law:

$$\hat{n}_I \sin\theta_I = \hat{n}_T \sin\theta_T. \tag{3.53}$$

The irradiance (or radiant flux density) of an electromagnetic beam is given by:

$$I = \frac{v\epsilon}{2} E_0^2, \tag{3.54}$$

where v and ϵ are the velocity and permittivity within the medium in which the beam is propagating. If one defines I_I, I_R, and I_T as the incident, reflected and transmitted irradiance of the beam, with corresponding areas normal to its direction of propagation of $A\cos\theta_I$, $A\cos\theta_R$, and $A\cos\theta_T$ respectively, then from the definition of power being the flux density multiplied by the cross-section over which the beam is acting, one can write the transmittance as:

$$\mathbf{T} = \frac{I_T \cos\theta_T}{I_I \cos\theta_I} \tag{3.55}$$

where the transmittance has been defined as the ratio of the transmitted over the incident power. Using the fact that $v^2 = \frac{1}{\mu\epsilon}$ and $\hat{n} = \frac{c}{v}$ equation 1.57 becomes:

$$\mathbf{T} = \frac{\hat{n}_T \cos\theta_T}{\hat{n}_I \cos\theta_I} t^2 \tag{3.56}$$

where

$$t = \frac{E_{0T}}{E_{0I}}. \tag{3.57}$$

Note, that at normal incidence, $\theta_T \approx \theta_I = 0$. The transmission coefficient, t, is obtained by consideration of the Fresnel equations which are treated in most texts concerning

optics or the optical properties of materials.[18, 20, 21] For normal incidence, at the interface between two media as considered above,

$$t = \frac{2\hat{n}_I}{\hat{n}_I + \hat{n}_T}, \tag{3.58}$$

which leads to:

$$\mathbf{T} = \frac{4\hat{n}_I\hat{n}_T}{(\hat{n}_I + \hat{n}_T)^2}. \tag{3.59}$$

For a larger system consisting of several boundaries between different media, the situation becomes much more complicated since one must consider reflection and transmission at each subsequent boundary, as well as take into account further complications such as multiple internal reflections. Although this will not be treated here, a discussion can be found in reference [14].

Chapter 4

Transmission of Superconducting Lead Films

4.1 History of Superconductivity

In 1911, Kamerlingh Onnes observed that when mercury is cooled to a sufficiently low temperature, its electrical resistance suddenly dropped to zero at 4 K. Observation of this phenomenon, now referred to as superconductivity, required temperatures of the order of liquid helium until the discovery of the cuprate superconductors in 1986. These materials exhibit superconductivity at temperatures of the order of 100 K.[22] As Kamerlingh Onnes found, as the temperature is lowered, the material eventually reaches a critical temperature, T_C, at which point it undergoes a phase transition from what is known as the normal state, T_N, where electrical resistivity is nonzero, to the superconducting state where the electrical resistivity is zero.[23]

A second defining characteristic of superconductors is the presence of the 'Meissner Effect'. Discovered in 1933 by Meissner and Ochsenfeld, it was found that if a superconductor is cooled in a magnetic field to a temperature below T_C, then at T_C, the magnetic field is expelled from the bulk. This property can be seen in the phenomenon known as magnetic levitation. Magnetic levitation is, however, more easily understood from the point of view of the related property of flux exclusion. When a magnet is brought in close proximity of a material which is in the superconducting state, a current is induced within the surface of the superconductor according to the classical laws of electromagnetism. Because the superconductor has no resistance, this induced current continues

to flow even after the magnet has stopped moving. The induced current results in an induced magnetic field which will completely cancel the external magnetic field and the magnet then 'floats' above the superconductor. Note, however, that flux exclusion is simply a consequence of perfect conductivity. The 'Meissner effect' requires that before cooling either a time-varying or a static magnetic field present within the bulk of the superconductor will be 'expelled' as T_C is approached.[23, 19] This is known as perfect diamagetism.

4.2 Theory of Superconductivity

Theories to explain superconductivity have been put forth since its discovery, however, it wasn't until 1950 that Fröhlich presented what would be the key ingredients to develop a theory which today gives a satisfactory microscopic explanation of superconductivity. This was put forth by Bardeen, Cooper and Schrieffer in 1957. Fröhlich's idea began with the realization that in addition to the electron-phonon interaction that gives rise to electrical resistance in metals, another fundamental interaction is the electron-electron interaction which is transmitted by phonons.[24] The essence of his theory was that if an electron should be scattered, emitting a phonon in the process of this scattering, then another electron could absorb this particular phonon, and so, it too would be scattered. Fröhlich also predicted the isotope effect from his calculations, in other words, that T_C is proportional to $M^{-\frac{1}{2}}$, where M is the mass of the ion. This resulted from his calculations of the elastic vibrational frequencies which are of the form $(K/M)^{\frac{1}{2}}$ where K is related to the force constant. The reason Fröhlich's calculation failed to explain the phenomenon of superconductivity was that it used the perturbation method, whereas Bardeen, Cooper and Schrieffer, (BCS), used the more powerful technique of the variational method to solve the problem.[23, 24]

The BCS theory begins by describing an attractive electron-electron interaction which is mediated by lattice vibrations and results in the formation of electron pairs which condense into the superconducting state. The electrons in these so called Cooper pairs have opposite spins, and thus form a boson-like state. The pair of electrons are bound together with an energy of the order of 2Δ which in the BCS theory is given by

$$2\Delta = 3.53kT_C \tag{4.1}$$

where k is Boltzmann's constant. This amount of energy gives rise to a gap between the superconducting state and the normal excited state. This pair of electrons can be broken apart with a photon whose energy, $\hbar\omega$, is greater than 2Δ. However, if a photon has an energy which is less than 2Δ, it will not be absorbed and so it must either be reflected if the sample is thick, or if the sample is thin enough it may be transmitted. [19] It is thus possible to probe the superconducting energy gap of very thin superconducting films in the far-infrared region because of the very low energy scale of the incident photons. These measurements are conducted by first measuring the transmission of the film in the superconducting state, $\mathbf{T}_S$, and then by measuring the same film in it's normal state, $\mathbf{T}_N$. Ratioing the two sets of data yields $\mathbf{T}_S/\mathbf{T}_N$. This result can be compared with that predicted by theory.

The ratio of the superconducting state to the normal state transmission, $\mathbf{T}_S/\mathbf{T}_N$, for a superconducting film of given thickness depends on the electrical properties of the material which is being studied. The material specific electrical properties are described by the optical conductivity, $\hat{\sigma}$. As discussed in section 3.3 of chapter 3, concerning the optical properties of solids, the optical conductivity is a complex quantity and thus currents can flow both in and out of phase with the applied electric field. That is,

$$\hat{\sigma} = \sigma_1 - i\sigma_2. \tag{4.2}$$

This is true for both the superconducting and the normal states, however, for the normal state, $\hat{\sigma}$ is approximately real and constant and so is referred to as σ_N. Consider, a plane wave in free space incident on a film of finite thickness, d, where $d \ll \lambda$, and λ is the wavelength of the incident light. The film is deposited on a substrate of infinite extension whose index of refraction is n and which is backed by free space. If reflections within the substrate are neglected, then the transmission, $\mathbf{T}$, through the film/substrate system can be approximated by:

$$\mathbf{T} = \frac{1}{|1 + \sigma d \frac{Z_0}{n+1}|^2} \tag{4.3}$$

where $Z_0 = 377\Omega$, is the impedance of free space.[25] Ratioing an expression of this form for the superconducting state to one for the normal state, gives:

$$\frac{\mathbf{T}_S}{\mathbf{T}_N} = \frac{1}{[\alpha]^2 + [\beta]^2} \tag{4.4}$$

where

$$\alpha = [\mathbf{T}_N{}^{\frac{1}{2}} + (1 - \mathbf{T}_N{}^{\frac{1}{2}}(\frac{\sigma_1}{\sigma_N})] \tag{4.5}$$

$$\beta = [(1 - \mathbf{T}_N{}^{\frac{1}{2}}(\frac{\sigma_2}{\sigma_N})]. \tag{4.6}$$

The quantities $\frac{\sigma_1}{\sigma_N}$ and $\frac{\sigma_2}{\sigma_N}$ have been calculated within BCS theory by Mattis and Bardeen. [26] By incorporating a Fortran subroutine to determine these quantities, provided by E. J. Nicol, based on reference [27], a program was written to calculate the ratio of $\mathbf{T}_S/\mathbf{T}_N$ at a reduced temperature, $T_{red} = \frac{T}{T_C}$, for a film of normal state dc conductivity, σ_N, thickness, d, deposited on a substrate of refractive index n. Some curves which have been calculated by the above method are shown in figure 4.1. Attention should be given to the fact that as the film thickness is increased, the maximum in the ratio of $\mathbf{T}_S/\mathbf{T}_N$ also increases. It should also be noted that as the film thickness is increased, the maximum shifts slightly to higher energies. The normal state transmittance of each film is listed along with its thickness.

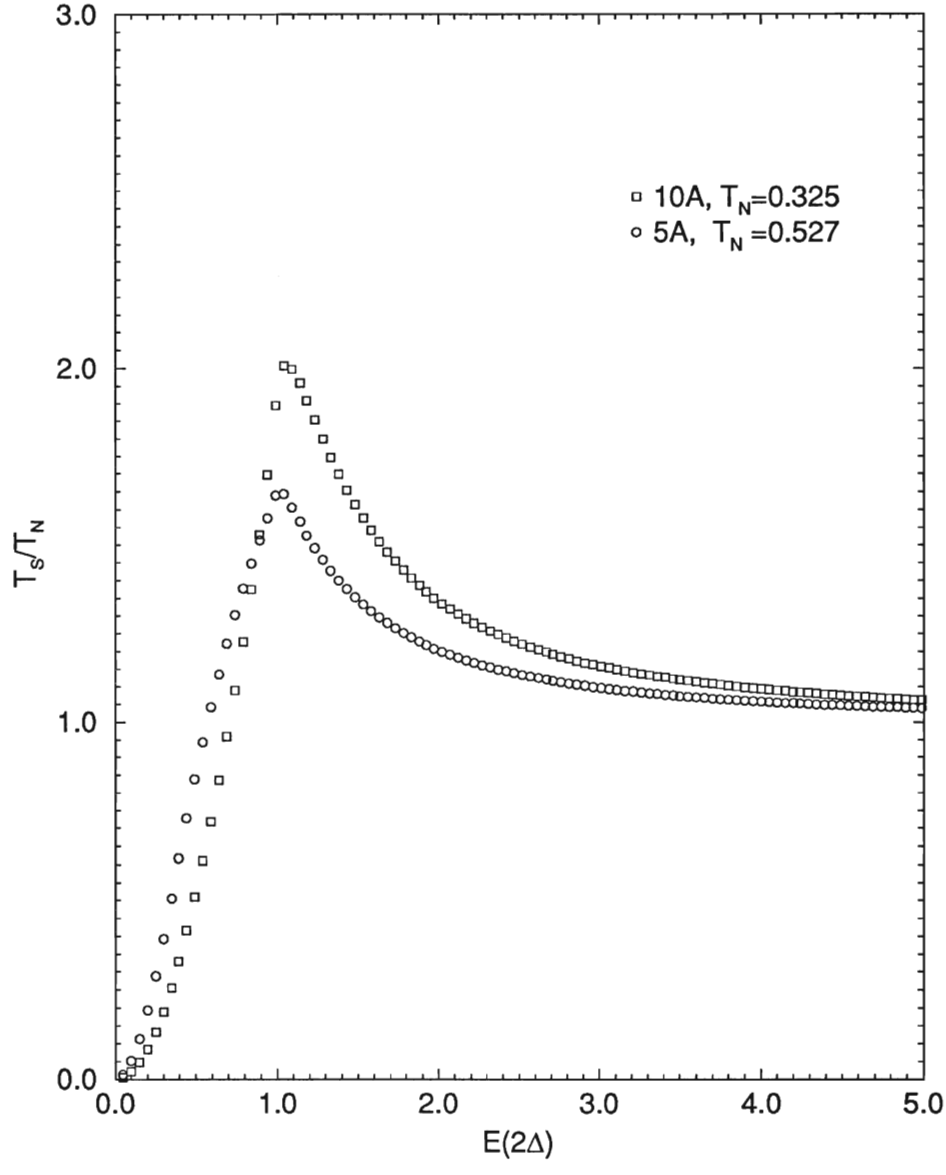

Figure 4.1: Simulated curves for films of various thickness at a reduced temperature of 0.07 where the index of refraction of the substrate is n=1.5, and the normal state resistivity of the film is $\rho = 20\mu\Omega$cm.

4.3 Literature Survey

Results for the transmission ratio of superconducting thin films of lead were first reported by Glover and Tinkham in 1957, [25]. Since Fourier transform spectroscopy was not yet available, the data was obtained through the use of a submm monochromator designed for use between 0.1 and 0.75 mm, with a mercury arc source. The instrument used 12 inch diameter optics and a Golay detector. Lock-in detection was used where the input chopper frequency was 10 Hz with a one minute time constant. Signals were averaged for one hour. The measurements were made on films which were approximately $20\dot{A}$ in thickness. Although large uncertainties were present, the raw data did show the influence of the energy gap. Tinkham then collaborated with Ginsberg in 1960 [28] and looked at a variety of different thin films, including lead. Results were obtained which agreed with those found in 1957. However, due to improvements in the system, these new results were believed to be much more accurate. Improvements to the system included the use of lightpipes to guide the radiation into the sample dewar, and a cooled carbon bolometer as a detector. In 1968, Palmer and Tinkham published more data on thin lead films [29], which included both transmission and reflectance measurements, further improving their signal-to-noise ratio. It was from these results that they noted σ_1 behaved as predicted by BCS theory, while, σ_2 did not. This problem was resolved by appealing to the strong coupling theory of superconductivity where the electron-phonon interaction is more pronounced than in the BCS approach.

Other work has been performed on lead films by a variety of different researchers.[30] This work focused mainly on the absorption in a variety of different geometries. Although this is interesting, the main thrust was to investigate the phonon structure in lead, well above the gap. Since this is not the focus of this chapter, comparisons herein will be made to the work of reference [25].

4.4 Transmission of Thin Films

The conventional superconductor, lead, was chosen to be studied since it has an easily obtainable critical temperature of 7.2 K[19]. Transmission measurements were carried out on three thin lead films of different thickness which have been deposited on quartz substrates.

4.4.1 Sample Preparation of Superconducting Films

The preparation required for carrying out a measurement of the transmission of a thin lead film in the very-far-infrared region consists of two steps: deposition of the film on an appropriate substrate, and mounting of the film inside the cryostat in a geometry such that the measurement can be made.

4.4.2 Evaporation Technique for Preparation of a Thin Film

The technique chosen for deposition of the lead to create thin films was evaporation. Fused silica quartz was chosen as the substrate material because of its availability and high transmittance below 100 cm^{-1}. The quartz substrates used were either 3/4" in diameter and 1/16" in thickness or 1" in diameter and 1/8" in thickness. Each substrate was cleaned with soap and water, rinsed with acetone and deionized water, and blown dry with air. The substrate was placed on the evaporator stage with a small piece of double sided tape and set over a dimpled tungsten ribbon filament into which an appropriate mass of lead was placed. Based on the previous work of reference [25], a film of approximately $20\dot{A}$ was required. If one assumes that the lead, when evaporated, deposits in a spherical pattern, then one can calculate the thickness of the film from:

$$t = \frac{m}{4\ \pi\ r^2 \rho} \tag{4.7}$$

where t is the thickness of the film, r is the distance between the substrate and the dimpled filament, $\rho = 11.35 g/cm^3$ is the mass density of lead [31], and m is the mass of lead used. The value of d was kept approximately constant at 10 cm. This approach, although useful as a first approximation, yielded films that were much too thin. It was known that the resulting films should have a resistance of the order of $200\Omega/\square$, while those created under the above described conditions had a resistance across the length of the substrate which was too large to be measured with an ordinary hand-held multimeter. The mass of lead was then increased by trial and error to obtain a film which measured 250Ω over a length of 1cm. A far-infrared transmission experiment was carried out on this film with the results reported as 'run 1'. As discussed in section 4.7, the far-infrared measurement indicated that this film was still quite thin. A second film was then made which measured 60Ω over a 1cm distance. This film was opaque to far-infrared radiation (run 2). Finally, a third film with a resistance of 140Ω over a 1cm distance was measured (run 3). The mass of lead used to make each film, the diameter of the substrate used, d, and the film resistance over a 1cm distance are summarized in table 4.1.

The films were made in a Varian Vacuum Evaporator SP 10E with an ac current of 60A. The length of the evaporation was approximately three hours, 2.75 hours to pump the system down to the lowest possible pressure and approximately fifteen minutes to evaporate, allow to cool and return the film to atmospheric pressure.

If one assumes that the current from the multimeter flows roughly through a square centimeter, and that the lead film is of uniform density, then from the standard resistivity formula,

$$\rho = \frac{RA}{L} \tag{4.8}$$

one can set the area, A, equal to tW where t is the thickness and W, the width, which

Run	Lead (g)	d	R/d	R/cm
1	0.01075 g	0.75"	$450\Omega/0.75$"	$250\Omega/cm$
2	0.01139 g	0.75"	$120\Omega/0.75$"	$60\Omega/cm$
3	0.01100 g	1.0"	$350\Omega/1.0$"	$140\Omega/cm$

Table 4.1: **Summary of some parameters pertaining to the lead films used for each of the three runs. Column two gives the mass of lead evaporated, column three gives the substrate diameter. Column four gives the resistance measured across the substrate, while column five gives that across a 1cm distance.**

for a square sampling area is also equal to L, the length. Therefore,

$$t = \frac{\rho}{R} \tag{4.9}$$

where ρ is the known resistivity of lead at room temperature, $\rho = 20\mu\Omega cm$[31], and, R, is the resistance measured over the 1 cm distance. The thickness, t, can thus be estimated as listed in table 4.2.

4.5 Resistivity Measurements

After completion of the far-infrared transmission experiment, a two-contact resistance measurement was carried out on the third film to confirm that it was indeed superconducting at low temperatures. This measurement was accomplished by silver-painting two fine wires onto the film and then gluing the substrate onto the resistance probe. The fine wires were soldered to copper pads from which more robust copper wires, fed through the probe, were connected to a Fluke 75 multimeter so that the resistance could be monitored as the probe was lowered into a cold helium storage dewar. The resistance was observed to drop from a value of 260Ω to 4Ω. The initial resistance of the film was determined by the separation of the contacts which could not be placed on the very edge of the

film because of the previous far-infrared mounting process. The resistance did not drop below 4Ω because that is the resistance of the contacts and the two copper wires which have been fed through the probe. From this measurement, the film has been shown to be, in fact, superconducting. For a more detailed explanation of the construction of the two-contact probe, see Appendix B.

4.6 Far-Infrared Measurement Technique

The thin film was silver-painted to an 'arm' constructed of copper as shown in figure 4.2. The arm was orientated so that the film was directly in front of the opening of the lightpipe leading to the bolometer, inside the cryostat. It was necessary to place the film here in order to best shield the bolometer from stray light and to avoid blocking incoming light. Absorption foam was used inside the sample chamber to eliminate light leaks, as described in chapter 2. The elimination of all light leaks is confirmed by the fact that in run 2 where the film was too thick, no signal could be detected. The foot of the arm was secured to the sample stage cold plate. In this way, it was believed that the arm would conduct the cold temperatures of the sample stage to the film. The light after having passed through the incident lightpipe was then focused with fused silica quartz lenses onto a large gold mirror which was glued to a holder placed on the sample stage, and reflected to the thin superconducting film.

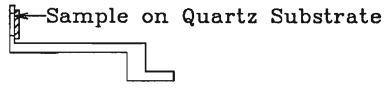

Figure 4.2: **Illustration of the 'arm' used for low temperature transmission measurements.**

4.7 Results and Discussion of Far-Infrared Measurements

Each far-infrared transmission measurement was conducted over approximately a twenty-four hour period. The lead film was deposited and mounted immediately in the cryostat, which was then evacuated for approximately eight hours. The standard procedure was followed to cool the cryostat and initiate data collection. The film was first measured in it's superconducting state. The temperature of the sample stage was 0.5 K. No intermediate reference could be used because the sample was placed directly in front of the bolometer. The power spectra were monitored to ensure that there was no significant drift with time. After sufficient data were obtained in the superconducting state, the sample stage was warmed using the Lakeshore Temperature Controller to $T_N = 12$K, a temperature well above T_C. Again, spectra were obtained and no reference was used. Finally, a temperature very close to T_C was measured. For this third temperature, the sample stage was cooled to 4.2K by using a heat switch to re-connect it with the helium-4 bath. It was then detached, warmed to 8K, and spectra were collected. As spectra were taken, the temperature fell to 6.8K. The stage was then warmed back to 8K and this process was repeated until sufficient spectra were obtained.

The data from runs 1 and 3 obtained by dividing the transmission through the film/substrate system in the superconducting state, $\mathbf{T}_S$, to that in the normal state, $\mathbf{T}_N$ is shown in figure 4.3. As was predicted by BCS theory, the presence of the energy gap is inferred from the peak-like structure of the ratio. Note that the maximum in $\mathbf{T}_S/\mathbf{T}_N$ for run 1 is quite low, indicating that this film is still quite thin, while that for run 3 is considerably higher as expected for a thicker film. Furthermore, as was noticed for the simulated curves in figure 4.1, a slight shift to higher frequencies of the maximum occurs in the experimental curves as the thickness of the film is increased. The ratio of the transmission of each film when it is at T_C divided by that when the film is at $\mathbf{T}_N =$

12 K is also presented in figure 4.3. As expected, this value is approximately equal to unity showing that in the normal state the optical properties are temperature independent. The maximum of the superconducting transmission ratio occurs between 25 - 26 cm^{-1}, from which one is able to determine an approximate value for $2\Delta/k_BT_C$. These results are summarized in table 4.2.

Run	R/cm	Peak Max.(cm^{-1})	I_{max}	$2\Delta/k_BT_C$	Thickness
1	250 Ω/cm	25	~ 1.1	5.0	$8\dot{A}$
2	60 Ω/cm	too thick	-	-	$33\dot{A}$
3	140 Ω/cm	26	~ 1.4	5.2	$14\dot{A}$

Table 4.2: **Summary of the results of the thin film transmission experiments. The first column gives the run number of the film measurement, column two gives the two probe resistance measured over a 1cm distance. Column three gives the position of the peak maximum in wavenumbers. Column four gives the maximum value of the transmission ratio. Column five gives the position of the peak maximum in units of $2\Delta/k_BT_C$ and the last column gives the thickness of the film obtained from the procedure described in section 4.4.2.**

The value of $2\Delta/kT_C$ estimated from the peak in $\mathbf{T}_S/\mathbf{T}_N$ is found to be approximately equal to 5.0, which is in reasonable agreement with references [25, 2]. This value is larger than the BCS weak-coupling prediction of 3.5, and indicates that the electron-phonon interaction for lead is in the strong-coupling regime.

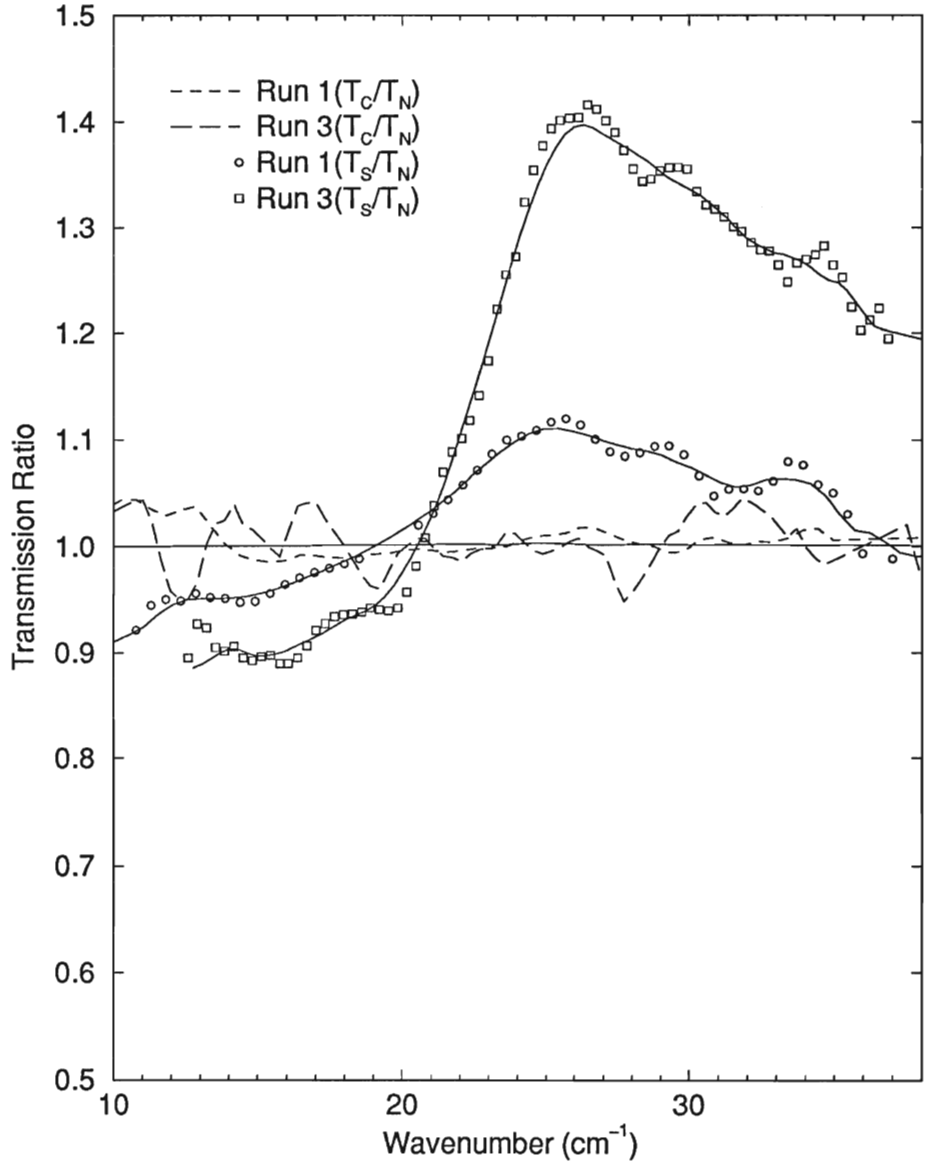

Figure 4.3: **Transmission ratios for two different thicknesses of thin lead films. Note that the peak maximum occurs at approximately 25-26cm^{-1}. The lines drawn through the experimental T_S/T_N points are guides to the eye.**

4.8 Conclusions

Superconducting thin films of lead were deposited and measured in the far-infrared by conducting transmission experiments. Based on the maximum in $\mathbf{T}_S/\mathbf{T}_N$, the energy gap of lead was found to be approximately 25 cm^{-1} which gives a value of $2\Delta/kT_C$ approximately equal to 5.0. These results are in good agreement with literature values, and illustrate the strong coupling nature of lead. The data presented here also showed that increasing the thickness of the film, leads to an increase in the ratio of $\mathbf{T}_S/\mathbf{T}_N$, in agreement with theoretical predictions and previous experimental work. From these results, it can be concluded that the far-infrared system that has been developed is operational and capable of measuring the superconducting state optical properties of low T_C superconductors.

Chapter 5

Transmission Studies of Water and Globular Protein Sols and Gels

The far-infrared transmission of the globular protein, Bovine Serum Albumin, has been studied in a variety of forms with the hope of gaining more information concerning thermal gels. Since water constitutes the basis for a protein in a hydrated form, its transmission was measured to provide a further check of the performance of the far-infrared system. The protein, Bovine Serum Albumin (BSA), was studied for various concentrations as an aqueous solution (sol) and in the form of a thermal gel, as well as in the crystalline state.

5.1 Theory of Transmission Measurements of Liquids

In order to understand the optical properties of liquid samples, one starts from the theory which was previously discussed in chapter 3. Recall, from equation 3.37 that a solution for the wave equation was given as:

$$\mathbf{E} = \mathbf{E}_0 e^{i(\mathbf{q}\cdot\mathbf{r}-\omega t)}. \tag{5.1}$$

The average electric field squared can then be calculated, resulting in:

$$|\bar{\mathbf{E}}|^2 = \mathbf{E}_0^2 e^{(-2q^* x)}, \tag{5.2}$$

for a one dimensional case where q^* is the imaginary component of the propagation vector,$\mathbf{q}$. However, from equation 3.54, one is able to state that

$$I \propto |\bar{\mathbf{E}}|^2 \tag{5.3}$$

which leads to the expression:

$$\frac{I}{I_0} = e^{-2q^* x}. \tag{5.4}$$

From the basic definitions of:

$$q = \frac{2\pi}{\lambda} \tag{5.5}$$

$$\lambda = \frac{v}{\nu} \tag{5.6}$$

$$v = \frac{c}{n}, \tag{5.7}$$

and

$$\bar{\nu} = \frac{\nu}{c} \tag{5.8}$$

the real part of **q**, the propagation vector can be written as:

$$q = 2\pi\bar{\nu}n. \tag{5.9}$$

Here, λ is the wavelength of the light, and v is the velocity in the medium of index, n. The quantity, c is the velocity of light in free space, and ν and $\bar{\nu}$ are its frequency in Hz and cm^{-1} respectively. From the requirement that q is a complex quantity, it is clear that we can write:

$$\mathbf{q} = 2\pi\bar{\nu}(n + ik), \tag{5.10}$$

where

$$q^* \equiv 2\pi\bar{\nu}k. \tag{5.11}$$

As stated in chapter 3 and from reference [14], one is thus able to write the transmittance as:

$$\mathbf{T} = \frac{I}{I_0} = e^{(-4\pi\bar{\nu}kx)}. \tag{5.12}$$

Solving for k one finds

$$k = -\frac{1}{4\pi\bar{\nu}x}\ln[\mathbf{T}]. \tag{5.13}$$

This is known as Lamberts law. A variation of this law known as Beers law is often used for solutions since in this case the absorption depends, not only upon the thickness traversed, x, but also on the total number of absorbing molecules, and hence upon the concentration, C. The end result is that k becomes:

$$k \equiv k_{intrinsic} C \tag{5.14}$$

where $k_{intrinsic}$ is the absorption coefficient for unit concentration. In practice, Beers law often does not hold since $k_{intrinsic}$ varies with concentration.[20]

5.2 Transmission Cell Preparation

In this section, the technique used to prepare the optical transmission cells will be described. The same procedure was followed for all samples studied, with some small modifications for examining the BSA crystals as will be described in section 5.6. The optical cells were made from two fused silica quartz windows separated by a spacer made from thin stainless steel. The stainless steel ring was epoxied to one quartz window using five minute epoxy. When the epoxy was dry, extra epoxy was removed with acetone, the liquid sample was placed inside the steel ring and more epoxy was placed near the outside edge of the ring. The second window was then placed on top of the ring. The second window was placed on the cell in such a way as to minimize the amount of air entering the cell. Fused silica quartz discs with a diameter of 1" and a thickness of 1/8" were used as the windows. The stainless steel ring had an inner diameter of 7/8", an outer diameter of 1" and a thickness of 3/1000". The sample holder made for the cell is shown in figure 5.1 while figure 5.2 illustrates its location in the far-infrared system.

Since the cell is located inside the lightpipe, it is clear that the measurements were performed under vacuum and at room temperature. The amount of epoxy used was kept to a minimum, and to ensure the cell was vacuum tight a thin layer of nail polish was

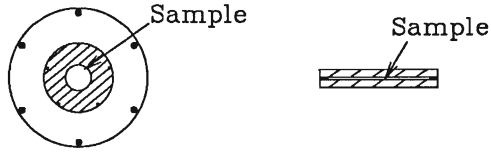

Figure 5.1: **The sample cell, composed of two fused silica quartz discs separated by a thin steel ring is placed inside a sample holder in the form of a vacuum flange.**

added to the outside perimeter of the cell. The cell was first vacuum-tested in a bell jar evaporator. If there was no change in the appearance of the cell after the bell jar had been evacuated to the lowest pressure possible with the roughing pump then it was assumed vacuum tight.

After the cell was constructed and tested, it was placed in the sample holder which doubled as a flange to connect the cryostat to the interferometer via the lightpipes. The MPI was then evacuated and measurements commenced.

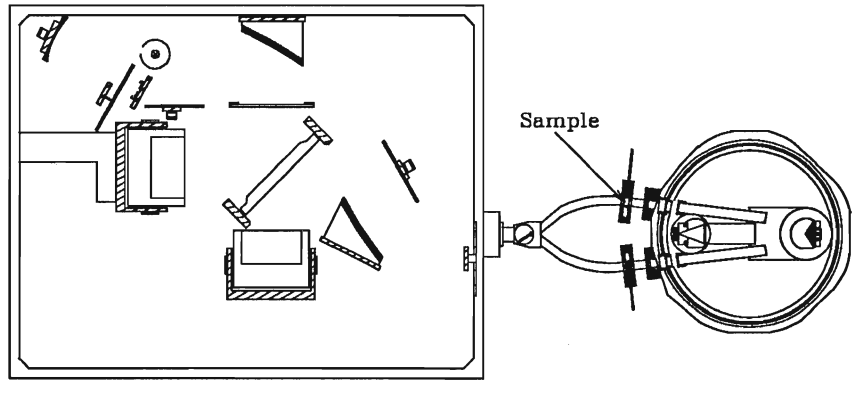

Figure 5.2: **Top view of the far-infrared system showing the location of the transmission cell. The flange containing the cell is used to connect the cryostat to the interferometer via the lightpipes.**

5.3 A Brief History of Infrared Measurements on Liquid Samples

The first record of a measurement carried out on a liquid sample in the infrared region was by Rubens in 1892.[14] He discussed the various quantities which can be extracted from transmission measurements. One of the samples which he studied was water. Through the years, water has been examined many times, in a variety of different ways. A summary of these studies is found in reference [14]. Renewed interest in the spectra of water occurred in the late 1950's and early 1960's during the advent of the space age. One of the consequences of remote sensing of planetary atmospheres and surfaces, was a renewed look at the optical properties of the earth's natural mineral resources. The most abundant resource, water, was thus studied in great detail. It should be noted that the relatively large static dielectric constant,

$$\epsilon = n^2 \tag{5.15}$$

is due to the strong polar nature and polarizability of water.

Since water is a major component of the sols and gels which were studied, it was also re-examined in this work, not to gain new insight into the material, but in order to illustrate the feasibility and accuracy of the transmission technique used. The data obtained will be compared to that given in reference [14].

5.4 Results and Discussion of Water Measurements

A transmission cell containing double deionized liquid water was constructed and mounted in the sample holder described in section 5.2. The standard technique for cooling the cryostat was followed. The detector used for this measurement was the 0.3 K bolometer with a crystalline quartz/diamond powder paste filter and fused silica lenses to give a cutoff near 100cm^{-1}. A standard technique in which the sample is measured and ratioed to an intermediate reference was used to collect data. The appropriate reference for the

sample, in this case an empty cell, is measured and ratioed to the same intermediate reference. The intermediate reference used was the open path in the other arm of the lightpipes. After both of these measurements have been carried out the transmission is obtained by calculating a final ratio of these two quantities:

$$\mathbf{T} = \frac{\frac{\mathbf{T}_{Sample}}{\mathbf{T}_{Int.Ref.}}}{\frac{\mathbf{T}_{Sample\ Ref.}}{\mathbf{T}_{Int.Ref.}}}. \tag{5.16}$$

The absorption coefficient was then extracted using the procedure described in section 5.1. As can be seen from figure 5.3, the experimental result obtained for water is in good agreement with the data taken from reference [14]. It should be noted that water is very absorbant in the far-infrared, and so very little radiation is able to propagate through the cell. This is why such a thin sample has been studied. As the thickness of the sample is increased, the amount of light which is able to propagate through the sample is reduced very quickly, until no signal can be detected. Note that since the epoxy changes the cell thickness, the actual thickness of the liquid sample is obtained by measuring the total thickness of the cell constructed and subtracting the thickness of the two quartz windows.

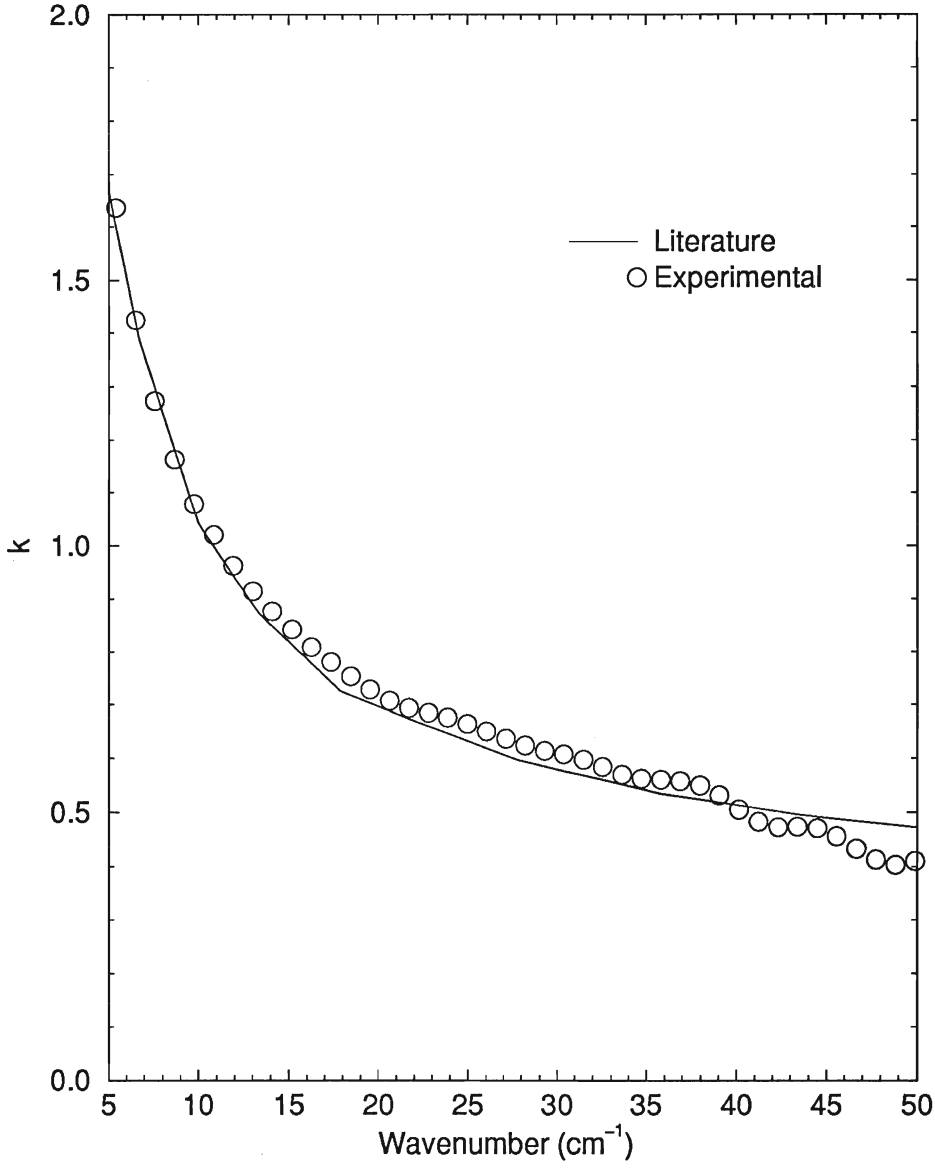

Figure 5.3: **The absorption coefficient, k as a function of wavenumber, $\bar{\nu}$ for double deionized water. Note the agreement with reference [14].**

5.5 Introduction to Proteins and Thermal Gels

Complex molecular structures are often intriguing to study. They usually provide a challenging problem which requires a great deal of thought and a detailed understanding of all aspects of the situation. Due to the complexity of proteins, they are an excellent example of this fact. Proteins which are required for all life processes are best described as a group of nitrogenous organic compounds of high molecular weight, synthesized by plants and animals, that upon hydrolysis by enzymes yield amino acids. [32] Proteins come in all shapes and sizes. The globular protein that has been studied here is Bovine Serum Albumin (BSA), and has a molecular weight of 66200. It is considered a smaller protein with quaternary structure. The structure of proteins can be considered on four levels: primary, secondary, tertiary and quarternary structure. Primary structure is normally defined as the sequence of peptide-bonded amino acids, including the location of the disulfide bonds and the covalent bonds between the amino acids themselves. This is the most basic structure of the protein. Secondary structure refers to the regular, recurring arrangements of amino acid sequences along the polypeptide. There are two common arrangements, namely the α helix and the β sheet conformations. Tertiary structure refers to the spatial relationship among all amino acids in a polypeptide. This is a complete three-dimensional structure. Finally, quaternary structure describes the spatial relationship of the polypeptides within the protein. Globular proteins, such as bovine serum albumin, often have many different types of secondary structures, and are very compact structurally. In other words, there is a great deal of folding in the tertiary structure.[33]

Denaturization of the protein structure can be accomplished in a variety of different ways, such as heating or via an additive. Through denaturization, one often demonstrates the importance of the specific structure and sometimes can determine it's function. This

denaturization is the main goal of thermal gels. The basic idea is to study the protein in solution, usually water. When the protein is hydrated and simply 'floating' in the water, it is referred to as a 'sol'. The second stage of the study is to heat the 'sol' so that a phase transition takes place, i.e. the proteins begin to unravel and form bonds between themselves, trapping the water. If this process is carried beyond the critical point then the protein will never be able to return to it's natural conformation. In this form, it is referred to as a 'gel'. [33]

5.6 Protein Sol and Gel Sample Preparation

In order to prepare the biological samples which were studied, double deionized water and bovine serum albumin were obtained. The bovine serum albumin, (BSA), was initially fractioned by heat shock, and was from Sigma Chemical Company, lot 102H0346. It's purity was greater than ninety-eight percent. All glassware and measuring devices were cleaned with soap and water, rinsed with acetone and distilled water, and blown dry with air. A variety of concentrations of bovine serum albumin (BSA) sol and gel were studied. All concentrations were determined by weight. The mass of the double deionized water was measured. After this, the BSA was weighed and sprinkled into the water. A spatula was used to stir the protein into the water so that it would take less time to dissolve. When all of the protein was in solution this was considered the BSA sol. The sols produced using this technique varied in their consistency. The low concentrations were similar to that of water and exhibited a pale yellow color. At higher concentrations a much more viscous liquid, exhibiting the same pale yellow color with a consistency similar to that of slime was obtained. To prepare the gel, the transmission optical cell containing BSA sol was placed in a beaker of 80°C water and 'cooked' for fifteen minutes. The water bath temperature oscillated between 78-82°C during this time. After the fifteen

minute time period, the cell was removed and placed in an ice bath for fifteen minutes and finally it was allowed to warm to room temperature.[34] The gel which formed was of a pale yellow color and varied in consistency from being somewhat viscous, similar to slime, for low concentration to a much more robust flexible plastic-like material at higher concentrations. The different concentrations were obtained by diluting the original concentration with water, or further concentrating by evaporation of the initial solution of 50% sol which had a pH of 8.

Crystals of BSA were also prepared by depositing a small quantity of BSA sol, 50% by weight, onto a fused silica quartz disc to which a stainless steel ring had been epoxied, and allowed to sit. Over an 8 hour time period, all of the water which was in solution appeared to evaporate, and crystals covered the substrate. These crystals were very thin and still exhibited the pale yellow color of the sol. A procedure similar to that of the liquid samples was used for mounting the transmission cell containing the crystals, however, instead of epoxying the stainless steel ring to both of the fused silica quartz discs, the second was attached with vacuum grease, in such a way as to allow air in the cell to be evacuated.

5.7 Literature Survey of Protein Measurements

Proteins have been studied for many years in a variety of different ways through the use of a multitude of techniques, however, very little work has been carried out on the low frequency optical properties. Interest in using far-infrared spectroscopy to probe proteins is developing, since this technique may be able to detect active vibrational modes without the sample size and data collection time restrictions of neutron scattering experiments. The optical properties of biological materials in this region of the electromagnetic spectrum are important because water is partially transparent and the frequency range

corresponds to thermal energies.[35] Furthermore, since the low frequency modes of vibration are generally affected by the protein structure, spectra in this region may be used to monitor conformational transitions occurring in solution.[36] Theoretical work has suggested that in this region of the spectrum,one might find evidence of longitudinal modes which play a role in biological processes [37] and of low frequency correlated motions of groups of atoms in the protein which are important in the thermodynamics of protein folding, activity and electron transport.[38]

Reference [39] reports on the spectrum of BSA, however, in a much higher frequency region. They claim that a broad peak observed in the absorption spectrum between 100 and 200cm^{-1} results from anharmonic coupling among soft modes, chiefly through H-bonded groups. The single broad band would result from the interaction of several levels.

Others have reported far-infrared measurements of globular proteins, [35, 36, 40, 41, 42], however, a direct comparison between the work presented here and that which has been published is difficult since it appears that no one has carried out measurements of BSA in solution at room temperature at such low frequencies. The only work to consider the effect of degree of hydration is that of [38] regarding the far-infrared absorption in lysozyme measured using synchrotron radiation. Compared to the solutions examined in this thesis, the levels of hydration in that study were very low.

5.8 Results and Discussion of Protein Measurements

5.8.1 Concentration Dependence of BSA sols and gels

Several concentrations of BSA sol were studied using the same experimental procedure and approach to analysis as was followed for liquid water. The results, which have been separated into two graphs for clarity, can be seen in figures 5.4 and 5.5. The first thing

that can be noted is that for all concentrations the frequency dependent absorption coefficient is smaller than that of water indicating that the protein solutions are more transparent than pure liquid water.

Figure 5.4 shows the frequency dependence of the absorption coefficient at concentrations obtained by diluting the initial 50% sol mixture. From these results, one can conclude that at these low concentrations, there is little change as the concentration is varied, and so it is clear that the simple linear dependence on concentration predicted by Beers law does not hold. Figure 5.5 shows the results obtained by evaporation concentration of the initial 50% sol mixture. A stronger concentration dependence is observed with the samples becoming increasingly more transparent as the concentration of BSA in solution rises. Some weak structure is observed in the frequency dependence of the absorption coefficient at all concentrations; most notably a broad hump near 20 cm^{-1}, and a gradual leveling off in the frequency dependence near 40 cm^{-1}. This feature near 20 cm^{-1} is in contrast to the results for water which showed at low frequencies, a monotonic decrease in k with increasing frequency and thus may result from low frequency vibrations of the hydrated protein molecules. These results are however preliminary, and further work should be carried out to rule out effects such as improper cancellation of interference effects due to the fact that the refractive index of the liquid sample is different from the vacuum reference, and that the magnitude of the discontinuity between the transmission medium and the cell windows is different for the sample and the reference.

Perhaps somewhat surprising, the results for the gel samples, shown in figure 5.6, are quite similar, showing that as the concentration of the gel increases, the value of the absorption coefficient decreases, indicating that the sample is more transparent. This could possibly be due to the water being absorbed by the protein while the protein is unfolding into it's three-dimensional matrix, but again, more detailed work is needed before definitive conclusions can be made. The weak structure observed in the frequency dependence

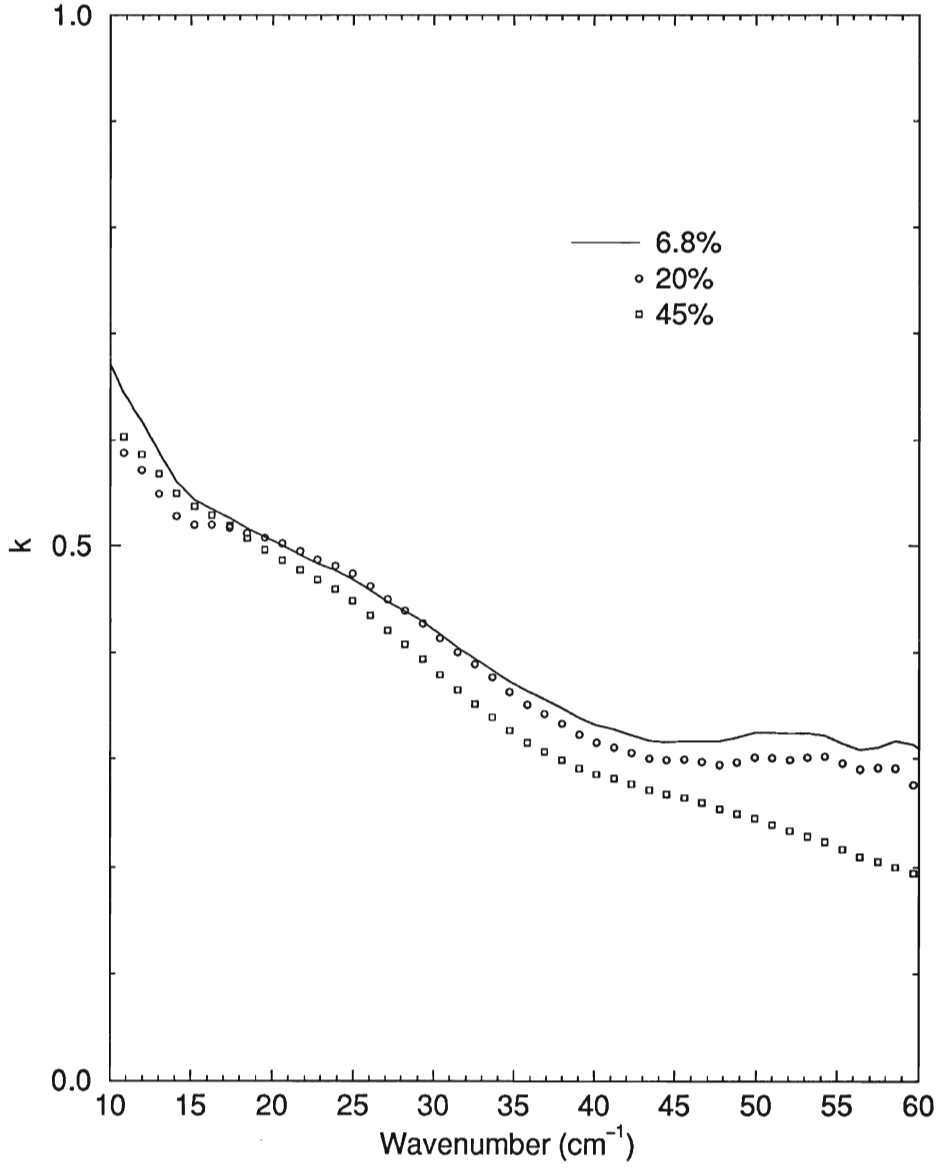

Figure 5.4: **The absorption coefficient, k as a function of wavenumber, $\bar{\nu}$ for low concentrations of BSA sol.**

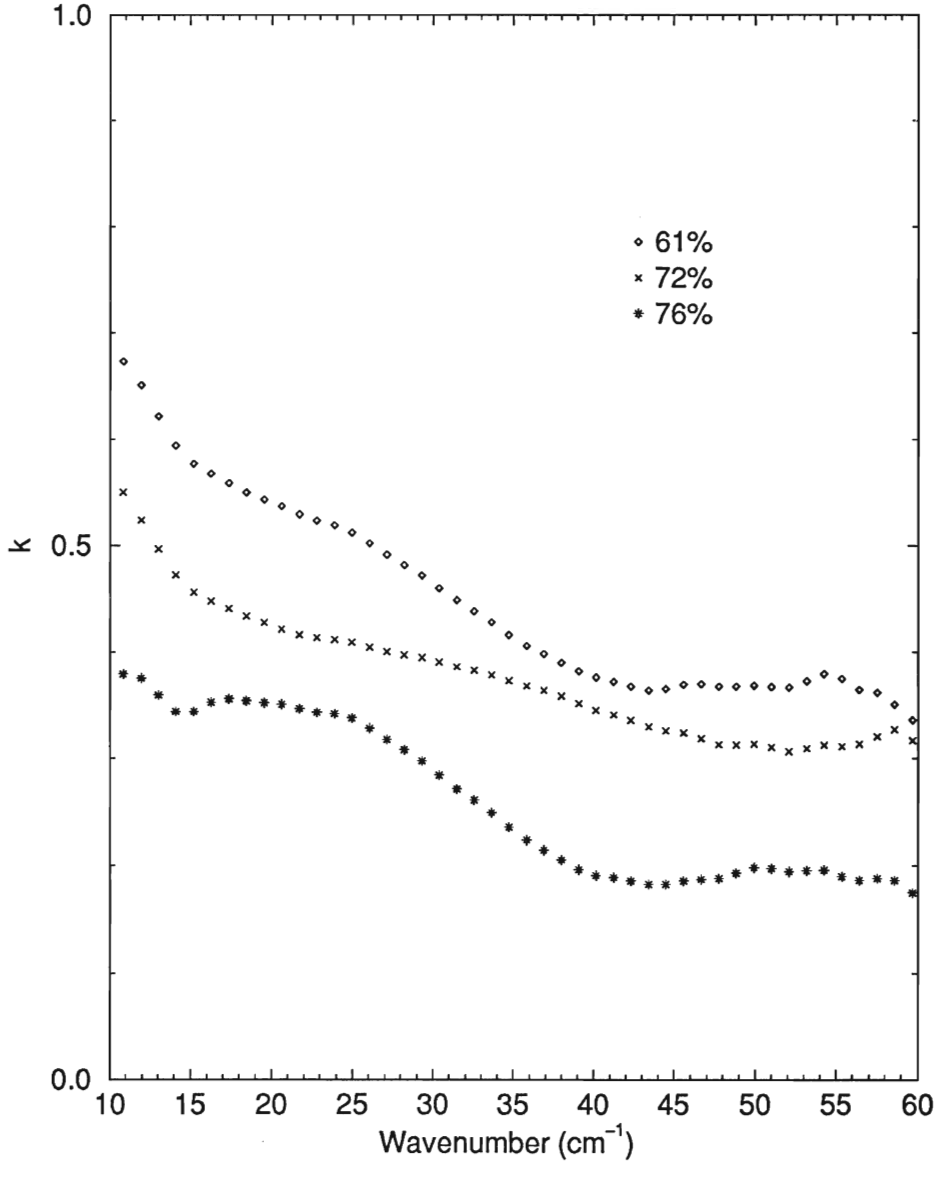

Figure 5.5: **The absorption coefficient, k as a function of wavenumber, $\bar{\nu}$ for high concentrations of BSA sol.**

of the absorption coefficient for the sol samples is also evident in all concentrations of the gel.

5.8.2 BSA Crystals

The absorption coefficient was determined for crystalline BSA which resulted from allowing 50% concentration by weight BSA sol to evaporate on a fused silica disc, as described previously. The results are shown in figure 5.7. In comparison to the sol and gel samples, the absorption coefficient is very small meaning that the radiation is able to propagate through the sample much more easily. Note the prominent absorption peak at approximately 48 cm^{-1}. There are also some smaller features at low frequencies, but it is possible that these may be due to improper cancellation of interference fringes. Ataka and Tanaka, in comparing their results for crystalline Lysozyme [42] with previous work of Buontempo et al. [35] also found considerably more prominent absorption structure. If one examines carefully the results for the sol and gel samples discussed in section 5.8.1, one notices that in the higher frequency region of the spectrum there is in many cases also evidence of some weak structure, indicating that this feature may indeed be due to low frequency vibrations of the protein molecules.

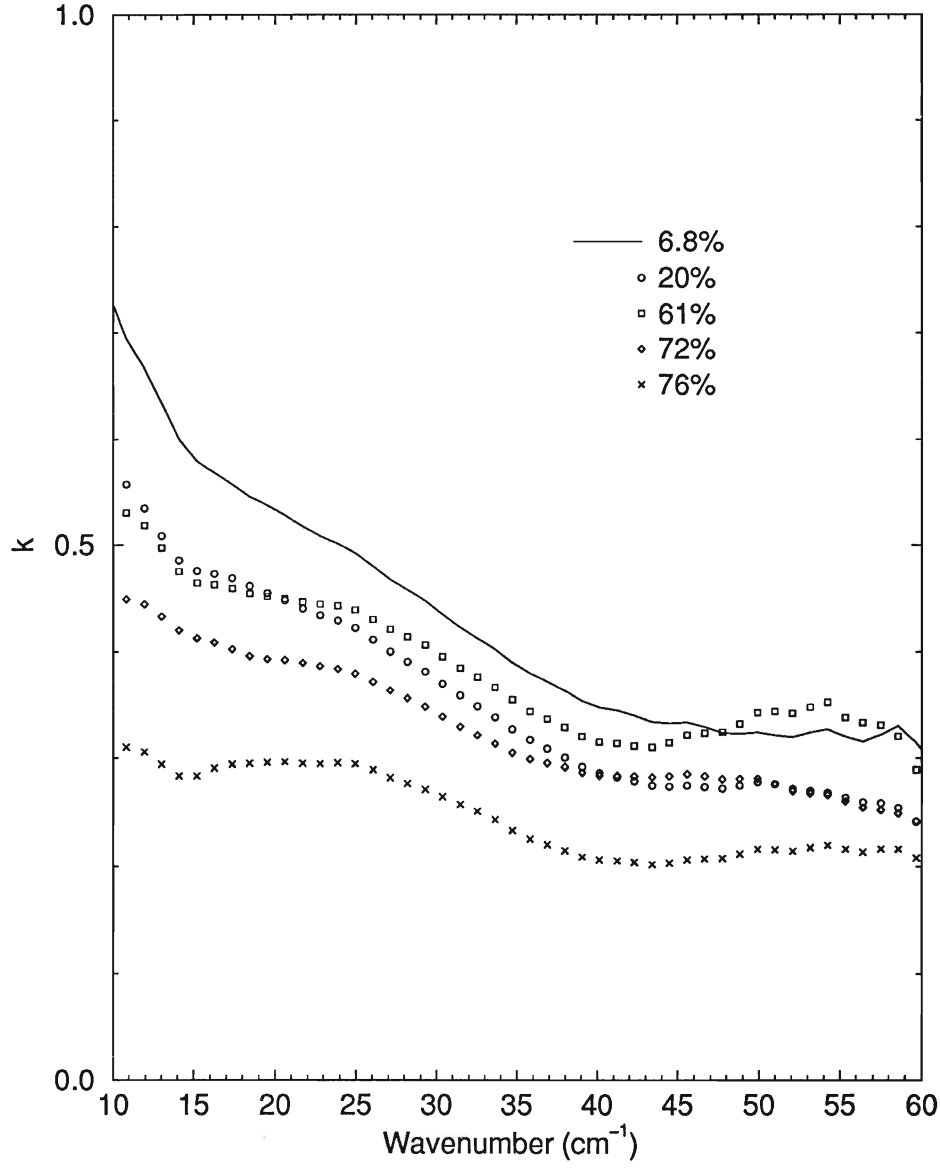

Figure 5.6: **The absorption coefficient, k as a function of wavenumber, $\bar{\nu}$ for various concentrations of BSA gel.**

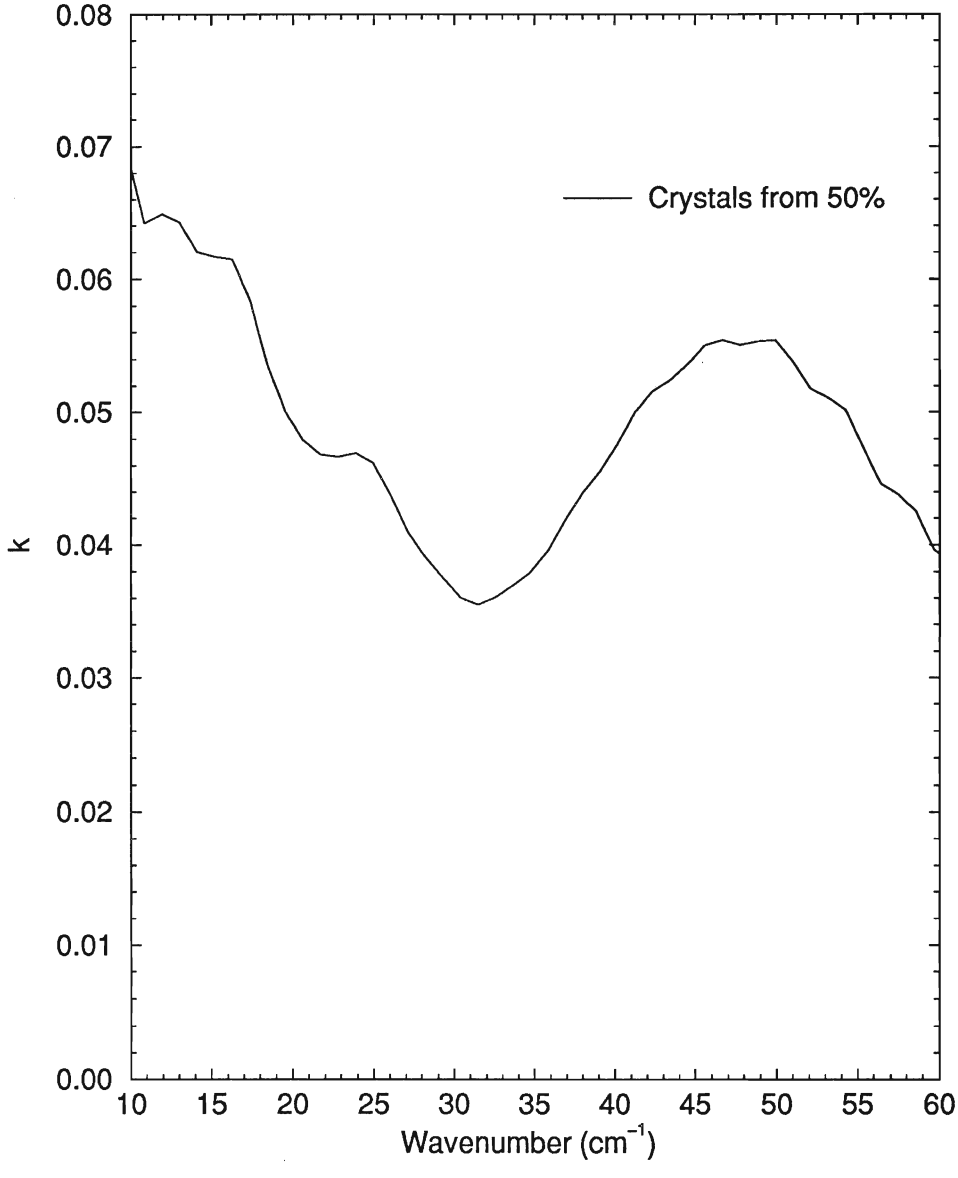

Figure 5.7: **The absorption coefficient, k as a function of wavenumber, $\bar{\nu}$ for crystals of BSA grown from 50% concentration by weight BSA sol.**

5.9 Conclusions

From the excellent agreement between the water data presented and that of reference [14], it is evident that the measurement technique used to study the liquid samples, is capable of producing reliable results. The frequency dependence of the absorption coefficient for the BSA sol and gel samples is smaller than that in water, and therefore they are more transparent than water in the far-infrared. There appears to be little concentration dependence for the lower concentrations of the sol, however with increasing concentration, some concentration dependence is observed. It has also been noted that some weak structure is observed in the absorption spectrum at 20 cm^{-1} and a leveling off, which may be due to the broad absorption peak observed in the crystalline sample, occurs near 40 cm^{-1}. This structure may be due to the low frequency vibrations of the hydrated protein molecules. From the detailed study of various gel concentrations, it is noted that the gels are somewhat more transparent than their corresponding sols, and that as the concentration of the gel increases, the value of the absorption coefficient decreases. It is suggested that this may be due to the water being absorbed by the protein while denaturation occurs and the three-dimensional matrix of the gel is being constructed. The BSA crystals were found to be much more transparent than the sol and gel samples and exhibited a prominent absorption peak near 48 cm^{-1}.

Chapter 6

Conclusions

6.1 Thin Superconducting Lead Films

Thin films of lead have been measured in the far-infrared region and the energy gap has been found to be approximately $25cm^{-1}$, which corresponds to $2\Delta/kT_C \sim 5$. This is in agreement with the results of references [25, 2]. The maximum in the ratio of $\mathbf{T}_S/\mathbf{T}_N$ was found to be 1.1 for a film which was approximately $8\dot{A}$ thick and 1.4 for a film which was approximately $14\dot{A}$ thick which conforms to the trend expected from theory. From these measurements, it may be concluded that the far-infrared system which has been developed is capable of measuring low T_C superconducting thin films.

6.2 Water and the Bovine Serum Albumin System

The frequency dependence of the absorption coefficient of water extracted from transmission measurements in the far-infrared region of the spectrum was found to agree well with literature values. In the preliminary measurements on the globular protein system, Bovine Serum Albumin, some concentration dependence of the transmittance in the far-infrared was observed for sol and gel samples. Weak structure has been observed in the frequency dependence of the absorption coefficient which may be due to low frequency modes of the protein. In the crystalline form the structure becomes much more pronounced. The results indicate that further study would be beneficial.

6.3 Final Remarks

In conclusion, it has been determined that this system which is capable of probing materials in the very-far-infrared region of the spectrum is providing accurate and reproducible results for the transmission of superconducting thin films of lead and for various liquids at room temperature. It is felt that the next step in determining the limitations of this system is to examine lower T_C thin superconducting films in order to establish the low frequency and temperature limits of the system. Further investigation of thermal gel samples including other globular proteins, is also warranted.

Appendix A

Controlling Program

This is a copy of the controlling program which was used before the C++ version was written. It has been modified from it's original version so that the lockin-amplifier can be automatically read and also so that the interferogram can be plotted in real time. The lines which have been added by the author are marked at the end of the line with "'*". All other lines have been directly taken from the program which was provided by SCIENCETECH, INC. [43]

```
10 CLS
20 '.........................Program "POLRUN"..............................
30 '                          SCIENCETECH INC, 1987
40 'Revised September 1989 for VAX: converted from QuickBasic to std.Basic.
50 'Revised March 1995: V2.0.............................................
60 'This program sets the data acquisition system for an interferometer
70 'with stepper motor drive.
80 'The user has to input the required resolution and cutoff and if it wants
90 'the interferogram to be symmetric or asymmetric.
100 'The program calls two subroutines: subroutine ZERO looks for the
110 'central max. and sets it position with respect to the limit switches.
120 'Subroutine INIT calculates the scanning parameters for a desired
130 'resolution and cutoff and recalculates them if necessary.
140 'Drives for external data acquis. systems must be implemented by the user
150 '.....................................................................
160 'Last modified in February 1996 by Katarin Baskin*
170 'Define fixed parameters
180 MECSTEP = .0001    'Mechanical half step set by the scanning system in cm.
190 NPRMAX = 8192      'Maximum number of right pts. that can be processed.
200 NPRMIN = 16        'Minimum number of right pts. that can be processed.
210 NPLMIN = 16        'Minimum number of left pts. that can be processed.
```

```
220 NPMAX = 4096       'Maximum number of total pts. that can be processed.
230 LIMIT = 5          'Distance from left to right switches in cm.
240 SAFEDIST = .1      'Safety distance to limit switches in cm.
250 NSTEPBL = 40       'Number of extra mechanical steps to avoid backlash.
255 ' changed backlash from 40 to 15 steps -- oct 19 1995
260 MEASTIME = 1      'Data acquisition time in seconds.
270 WAITIME = 2        'Settling time from step to read in seconds.
280 CHOPFREQ = 19      'Chopper freq. in revs./sec. (cycles=2*rev/sec).
285 POWERTWO = 1
286 ' note: added the above line -- appeared to be missing -oct 19 1995
287 ' probably adds zeroes to the ends of the interferogram?
290 'the right for the FFT as a power of two. Change to zero if algorithm
300 'does not require the number of data points as a power of two.
310 MICRFLAG = 1       'Convert to 0 for debugging without microprocessor
320 '.....................................................................
330 'Convert to microprocessor units
340 MEASTIME = MEASTIME * 10: WAITIME = WAITIME * 10
350 IF MEASTIME > 255 THEN PRINT "Data acquisition time too long": STOP
360 IF WAITIME > 255 THEN PRINT "Delay time too long": STOP
370 '.....................................................................
380 'Read old central maximum and define the position of the end switches
390 OPEN "zero.dat" FOR INPUT AS #3
400 INPUT #3, CENTER
410 CLOSE #3
420 PRINT "Latest zero position ="; CENTER
430 LIMITL = MECSTEP * ABS(CENTER)
440 LIMITR = LIMIT - LIMITL
450 '
460 '*********************************************************************
470 'The parameter INTREAD defines whether the instrument reads internally
480 '(INTREAD=1) or from an external instrument (INTREAD=0)
490 INTREAD = 0
500 '*********************************************************************
510 'Array definitions
520 IF MICRFLAG = 0 GOTO 900
530 DIM interf(NPMAX)
540 '
550 'Open communication with microprocessor
560 GOSUB 4270
570 '
580 'Initialize microprocessor with settling wait time.
```

```
590 A1$ = "W" + CHR$(INT(WAITIME))
600 PRINT #2, A1$
610 A2$ = INPUT$(2, #2)
620 IF A2$ = A1$ GOTO 660
630 PRINT "There has been a communication error at settling time init."
640 PRINT "Returned message: "; A2$
650 STOP
660 INPUT #2, A2$   'Clear buffer
670 'Set chopper speed
680 TAU0 = 3.2552E-05
690 PERIOD = 1 / (CHOPFREQ * TAU0)
700 PERIOD1% = INT(PERIOD / 256)
710 PERIOD2% = INT(PERIOD - 256 * PERIOD1%)
720 A1$ = "C" + CHR$(PERIOD1%) + CHR$(PERIOD2%)
730 PRINT #2, A1$
740 A2$ = INPUT$(3, #2)
750 IF A2$ <> A1$ THEN PRINT "There has been a communication error: "; A2$: STOP
760 INPUT #2, A2$   'Clear buffer
770 PRINT "Please wait: ramping chopper"
780 'Error trapping: It returns to the controlling program if the
790 'instruction has been completed succesfully. Otherwise it gives an
800 'error mesagge and stops
810 INPUT #2, A$
820 IF A$ = "CD" THEN PRINT "Chopper at desired speed": GOTO 850
830 IF A$ = "EC" THEN PRINT "Chopper unlocked": STOP
840 PRINT "Unrecognized message: "; A$: STOP
850 GOSUB  4320                 'Open communication with DVM
860 '
870 GOSUB  2960                 'Look for central maximum
880 '
890 '.....................input variables ............................
900 PRINT : INPUT "Cutoff (cm-1) ? ", CUTOFF
910 INPUT "Resolution (cm-1) ? ", RESOLUT
920 ASSYF = 1
930 PRINT "Symmetric interferogram ? (press y or n) ";
940 A$ = INKEY$: IF A$ = "" GOTO 940
950 PRINT A$
960 IF A$ = "n" OR A$ = "N" THEN ASSYF = .2: GOTO 980
970 IF A$ <> "y" AND A$ <> "Y" GOTO 930
980 GOSUB  2070                 'Calculate all parameters
990 PRINT
```

```
1000 PRINT "Corrected cutoff ="; ACUTOFF
1010 PRINT "Corrected resolution ="; ARESOLU
1020 PRINT "Total number of sampling points ="; npoints
1030 PRINT "Number of points to the right of central maximum ="; NPRIGHT
1040 PRINT "Number of points to the left of central maximum ="; NPLEFT
1050 PRINT "Number of mechanical steps per sampling data ="; nsteppp
1060 PRINT
1070 PRINT "Parameters adequate for scanning ? (press y or n) ";
1080 A$ = INKEY$: IF A$ = "" GOTO 1080
1090 PRINT A$
1100 IF A$ = "n" OR A$ = "N" GOTO 900
1110 IF A$ <> "Y" AND A$ <> "y" GOTO 1070
1120 'Initialize microprocessor with length of interval
1130 A1$ = "S" + CHR$(nsteppp)
1140 GOSUB 4270
1150 PRINT #2, A1$
1160 A2$ = INPUT$(2, #2)
1170 CLOSE #2
1180 IF A2$ <> A1$ THEN PRINT "There has been a communication error: "; A2$: STOP
1190 INPUT "Number of passes per scan ? ", NSCANS
1200 INPUT "Number of scans ? ", FILEND%
1210 FILENUM% = 1
1220 INPUT "First part of filename (up to 7 chars) ? ", filenam$
1230 PRINT "Ready to scan ? (press y or n) ";
1240 A$ = INKEY$: IF A$ = "" GOTO 1240
1250 PRINT A$
1260 IF A$ = "N" OR A$ = "n" GOTO 990
1270 IF A$ <> "y" AND A$ <> "Y" GOTO 1230
1280 '..... Scanning.....
1290 'Go to starting point for scan. Move mirror from central maximum to
1300 'the left NPLEFT*NSTEPPP steps.+backlash
1310 ZDISPL = -(NPLEFT * nsteppp + NSTEPBL)
1320 GOSUB 3650
1330 ZDISPL = NSTEPBL
1340 GOSUB 3650
1350 FOR j = 1 TO NSCANS
1360 GOSUB 4270
1370 FOR istep = 1 TO npoints + 2
1380 'added +2 to npoints above to include a point at the zeropath
1390 'and an extra to account for finding the maximum in the fft prog
1400 interf(istep) = 0
```

```
1410 NEXT istep
1420 'Start scanning: steps NPOINTS intervals and reads internal or
1430 'external signal
1440 GOSUB 4440
1450 interf(1) = interf(1) + zvalue
1460 GOSUB 4660
1470 istep = 1
1480 GOSUB 5270
1490 FOR istep = 2 TO npoints + 2
1500 'added +1 to npoints to include a point at the zeropath
1510 'and an extra to account for finding the maximum in the fft prog
1520 GOSUB  3940                    'Go to Subroutine Step
1530 GOSUB  4340                    'Read
1540 interf(istep) = interf(istep) + zvalue
1550 ' IF INT(ISTEP / 1) = ISTEP / 1 THEN PRINT ISTEP;
1560 GOSUB 5270
1570 NEXT istep
1580 CLOSE #2
1590 CLS
1600 PRINT : PRINT "Pass # "; j; " Scan # "; FILENUM%; " complete"
1610 'Returns to left (start) position plus backlash
1620 ZDISPL = -((npoints + 1) * nsteppp + NSTEPBL)
1630 GOSUB 3650
1640 ZDISPL = NSTEPBL           'Go to left (start) position
1650 GOSUB 3650
1660 NEXT j
1670 'Returns motor to central maximum position
1680 ZDISPL = (NPLEFT * nsteppp)
1690 GOSUB 3650
1700 FOR i = 1 TO npoints + 2
1710 'added 1 to npoints to account for point at zeropath
1720 'and 1 to account for finding max in fft program
1730 interf(i) = interf(i) / NSCANS
1740 NEXT i
1750 ' A$ = FILENAM$ + CHR$(64 + FILENUM%)
1760 A$ = filenam$ + ".dat"
1770 FILENUM% = FILENUM% + 1
1780 CLOSE
1790 OPEN A$ FOR OUTPUT AS #1
1800 PRINT
1810 FOR i = 1 TO npoints + 2
```

```
1820 nxb1 = -1 * npoints / 2 - 1 + i
1830 nxb1 = nxb1 * nsteppp * 2
1840 ' the factor of two converts it to optical (as opposed to
1850 '(mechanical) path difference.  Units are microns.
1860 WRITE #1, nxb1, interf(i): PRINT INT(1000 * interf(i) + .5);
1870 NEXT i
1880 PRINT : PRINT
1890 CLOSE
1900 IF FILENUM% < FILEND% THEN GOTO 1280
1910 IF FILENUM% = FILEND% THEN GOTO 1280
1920 PRINT "Run complete": PRINT
1930 CLOSE #4
1940 CLOSE #2
1950     FOR noise = 1 TO 2'*
1960     BEEP'*
1970     FOR length = 1 TO 100: NEXT length'*
1980     NEXT noise'*
1990 PRINT "Do you want to scan again? (y/n)"'*
2000 INPUT dumb$'*
2010 IF dumb$ = "y" OR dumb$ = "Y" THEN GOTO 10'*
2020
2030
2040 STOP
2050 END
2060 '.....................................................
2070 ' SUBROUTINE INIT
2080 '
2090 '.....................................................
2100 ' INITIALIZATION FTIR POLARIZING INTERFEROMETER
2110 ' SCIENCETECH Inc., 1987
2120 'Revised September 1989 for VAX: converted from QuickBasic to std. Basic
2130 '.....................................................
2140 'This subroutine calcs. the scanning parameters and closer resolution
2150 'and cutoff possible, determined by the drive system and the size of the
2160 'data array, from the requested values for the cutoff and resolution.
2170 '.....................................................
2180 '
2190 'RESOLUT and CUTOFF are given in cm-1. MECSTEP is in cm.
2200 'nsteppp=number of mechanical steps (MECSTEP) per sampling interval,
2210 'determined by the required cutoff according to Nyquist Criterion.
2220 nsteppp = INT(1 / (2 * 2 * CUTOFF * MECSTEP) + .5)
```

```
2230 'If cutoff too large, take the maximum that yields one sampling per
2240 'mechanical step.
2250 IF nsteppp < 1 THEN nsteppp = 1: PRINT "Cutoff too large"
2260 ACUTOFF = INT(100 / (2 * 2 * nsteppp * MECSTEP) + .5) / 100
2270 IF ABS(ACUTOFF - CUTOFF) > 1 THEN PRINT "New uncorrected cutoff ="; ACUTOFF
2280 '.........Determine actual resolution.................................
2290 'If Resolution too low, redefine it.
2300 RESMIN = (.2 * ACUTOFF)
2310 IF RESOLUT < RESMIN GOTO 2340
2320 RESOLUT = ACUTOFF / 10
2330 PRINT "Resolution too low, redefined in term of cutoff"
2340 'Calculate number of points at the right of the central maximum
2350 '(NPRIGHT) given by the resolution (no apodization)
2360 NPRIGHT = INT(ACUTOFF / RESOLUT + .5)
2370 'Check that the number is not too large or too small
2380 IF NPRIGHT < NPRMAX GOTO 2410
2390    NPRIGHT = NPRMAX
2400    PRINT "Resolution too high, number of points to the right decreased"
2410 IF NPRIGHT > NPRMIN GOTO 2440
2420    NPRIGHT = NPRMIN
2430    PRINT "Resol. too low, number of sampling pts.to the right increased"
2440 IF NPRIGHT > NPLMIN GOTO 2480
2450    NPRIGHT = NPLMIN
2460    PRINT "Resol. too low, number of sampling pts.to the right increased"
2470 '
2480 'Calculate the number of pts.at the left of the central maximum (NPLEFT)
2490 NPLEFT = INT(ASSYF * NPRIGHT)
2500 IF NPLEFT < NPLMIN THEN NPLEFT = NPLMIN      'too few?
2510 IF NPLEFT > NPRIGHT THEN NPLEFT = NPRIGHT    'too many?
2520 'If interferogram symmetric set points to the right same as to the left
2530 IF ASSYF = 1 THEN NPLEFT = NPRIGHT
2540 '
2550 '....Check if it does not hit the limit switch at the right within a
2560 '....safety distance determined by SAFEDIST
2570  DISTR = NPRIGHT * MECSTEP * nsteppp + SAFEDIST
2580 IF DISTR < LIMITR GOTO 2710
2590 NPRIGHT = INT((LIMITR - SAFEDIST) / MECSTEP / nsteppp)
2600 PRINT "Would hit right limit switch, resolution too high"
2610 PRINT "Total sampling points to the right decreased"
2620 'Check if points are not too few after adjustment
2630 IF NPRIGHT > NPRMIN GOTO 2660
```

```
2640    NPRIGHT = NPRMIN
2650    PRINT "Corrected number of points too small, resolution adjusted"
2660 IF NPRIGHT > NPLMIN GOTO 2690
2670    NPRIGHT = NPLMIN
2680    PRINT "Corrected number of points too small, resolution adjusted"
2690 NPLEFT = INT(ASSYF * NPRIGHT)'find points to the left
2700 IF NPLEFT < NPLMIN THEN NPLEFT = NPLMIN'check if they are not too few
2710 '
2720 '..Check if it does not hit the left limit switch within the safety
2730 '..dist. SAFEDIST, in this case change the resol. only if necessary.
2740 DISTL = NPLEFT * MECSTEP * nsteppp + SAFEDIST
2750 IF DISTL < LIMITL GOTO 2820
2760    NPLEFT = INT((LIMITL - SAFEDIST) / MECSTEP / nsteppp)
2770    PRINT "Would hit left limit switch, points to the left decreased"
2780    IF NPLEFT > NPLMIN GOTO 2830'check if points not too few after change
2790       NPLEFT = NPLMIN          'if they are, set them to the limit and
2800       NPRIGHT = INT(NPLMIN / ASSYF)'change resolution .
2810       PRINT "Resolution changed"
2820 '
2830 'If interferogram symmetric, set points to the right same as to the left
2840 IF ASSYF = 1 THEN NPRIGHT = NPLEFT
2850 '
2860 'Calculate total number of sampling points
2870 IF POWERTWO = 1 THEN NPLEFT = INT(2 ^ INT(LOG(NPLEFT) / LOG(2)) + .5)
2880 IF POWERTWO = 1 THEN NPRIGHT = INT(2 ^ INT(LOG(NPRIGHT) / LOG(2)) + .5)
2890 npoints = NPLEFT + NPRIGHT
2900 '
2910 'Print corrected values of resolution, cutoff and sampling points
2920 ACUTOFF = INT(100 / (2 * 2 * nsteppp * MECSTEP) + .5) / 100
2930 ARESOLU = ACUTOFF / NPRIGHT
2940 RETURN
2950 '.....................................................................
2960 '.......................SUBROUTINE ZERO.............................
2970 '                        SCIENCETECH INC,1989
2980 '.....................................................................
2990 'This subroutine allows the user to look manually for the position of
3000 'the central maximum of the interferogram for initialization of the
3010 'system and for alignment of the system. It first tells the stepping
3020 'motor controller to take the moving mirror up to the left limit
3030 'switch, then the user request the number of steps to be moved, after
3040 'each move the signal from the detector is read. The user can in this
```

```
3050 'way find the maximum position from the detector values. When this is
3060 'achieved it can set this position of the moving mirror as a zero for
3070 'the counting of sampling points. Any points to the right of the
3080 'central maximum will be positive, and sampling points to the left
3090 'will be negative.
3100 '.....................................................................
3110 PRINT "Are you close to the central maximum ? (press y or n) ";
3120 A$ = INKEY$: IF A$ = "" GOTO 3120
3130 PRINT A$
3140 IF A$ = "y" OR A$ = "Y" GOTO 3200
3150 IF A$ <> "n" AND A$ <> "N" GOTO 3110
3160 PRINT "Please wait while finding switch and going to zero path pos."
3170 GOSUB  3450                'Find left end switch
3180 PRINT "Please wait while moving to zero path"
3190 ZDISPL = CENTER
3200 GOSUB  3650                'Move to old zero position
3210 ZPOSIT = CENTER
3220 PRINT : INPUT "Displ.from last pos.(>0 for data)(0 to end) ? ", ZDISPL
3230 IF ZDISPL = 0 GOTO 3290
3240   ZPOSIT = ZPOSIT + ZDISPL
3250   GOSUB 3650'move
3260   GOSUB 4340'read
3270   PRINT "Pos ="; ZPOSIT; "Val ="; zvalue,
3280   GOTO 3220
3290 ABSPOS = 0
3300 'Define the new position of the end switches
3310 LIMITL = MECSTEP * ABS(ZPOSIT)
3320 LIMITR = LIMIT - LIMITL
3330 PRINT "Store new center in disk ? (press y or n) ";
3340 A$ = INKEY$: IF A$ = "" GOTO 3340
3350 PRINT A$
3360 IF A$ = "n" OR A$ = "N" THEN RETURN
3370 IF A$ <> "Y" AND A$ <> "y" GOTO 3290
3380 OPEN "zero.dat" FOR OUTPUT AS #3
3390 PRINT #3, ZPOSIT
3400 CLOSE #3
3410 CENTER = ZPOSIT
3420 RETURN
3430 '..................... End of subroutine zero .....................
3440 '
3450 '................... Subroutine to go to the end switch ..............
```

```
3460 'The "+" end switch is the closest to the beam splitter
3470 A1$ = "F+"
3480 PRINT #2, A1$
3490 INPUT #2, A2$
3500 IF A2$ = A1$ GOTO 3540
3510   PRINT "There has been a communication problem"
3520   PRINT "Returned message: "; A2$
3530   STOP
3540 PRINT "Waiting for end switch to be reached"
3550 INPUT #2, A2$
3560 IF A2$ = "+D" GOTO 3600
3570   PRINT "There has been a communication problem"
3580   PRINT "Returned message: "; A2$
3590   STOP
3600 PRINT "Found end switch as expected"
3610 CLOSE #2
3620 RETURN
3630 '.............. End of subroutine to go to the end switch ..............
3640 '
3650 'Subroutine to move the motor a given number of mechanical (half)
3660 'steps (ZDISPL) and to stop and give an error message if the end
3670 'switch is found.
3680 IF ZDISPL >= 0 THEN A1$ = "M-"
3690 IF ZDISPL < 0 THEN A1$ = "M+"
3700 ZDISPA = ABS(ZDISPL)
3710 ZDISP1% = INT(ZDISPA / 256)
3720 ZDISP2% = INT(ZDISPA - 256 * ZDISP1%)
3730 A1$ = A1$ + CHR$(ZDISP1%) + CHR$(ZDISP2%)
3740 ABSPOS = ABSPOS + ZDISPL
3750 GOSUB 4270
3760 PRINT #2, A1$
3770 A2$ = INPUT$(4, #2)
3780 IF A2$ = A1$ GOTO 3820
3790   PRINT "There has been a communication problem"
3800   PRINT "Returned message: "; A2$
3810   STOP
3820 INPUT #2, A$     'Clear buffer
3830 'Error trapping subroutine:
3840 'It returns to the controlling program if the instruction has been
3850 'completed successfully. Otherwise it gives an error message and stops.
3860 INPUT #2, A$
```

```
3870 IF A$ = "MD" THEN GOTO 3920
3880 IF A$ = "EC" THEN PRINT "Chopper unlocked": STOP
3890 IF A$ = "+E" THEN PRINT "Right end switch found": STOP
3900 IF A$ = "-E" THEN PRINT "Left end switch found": STOP
3910 PRINT "Unrecognized microprocessor message: "; A$: STOP
3920 RETURN
3930 '.............. End of subroutine to move the motor ..............
3940 '.....................................................................
3950 '.........................Subroutine step.............................
3960 'Moves the stage "I" intervals at a time and stops for a wait time,
3970 'in normal operation moves 1 interval at a time
3980 A1$ = "I-" + CHR$(0) + CHR$(1)
3990 GOSUB 3750
4000 INPUT #2, A$  'Clear buffer
4010 A2$ = INPUT$(2#, 2)
4020 INPUT #2, A$  'Clear buffer
4030 IF A2$ = "ID" THEN RETURN
4040 IF A2$ = "+E" THEN PRINT "Hit right limit switch": STOP
4050 IF A2$ = "-E" THEN PRINT "Hit left limit switch": STOP
4060 PRINT "Unrecognized microprocessor message: "; A2$: STOP
4070 STOP
4080 '..................Failsafe communications routine...................
4090 A2$ = ""
4100 FOR ICOM = 1 TO LEN(A1$)
4110    A$ = MID$(A1$, ICOM, 1)
4120    GOSUB 4180
4130    A2$ = A2$ + B$
4140 NEXT ICOM
4150 PRINT #2, ""
4160 IF A1$ <> A2$ THEN PRINT "Communication error: "; A2$: STOP
4170 RETURN
4180 'Output and input single character
4190 PRINT #2, A$;
4200 'Input single character
4210 IF LOC(2) = 0 GOTO 4210
4220 B$ = INPUT$(1, #2)
4230 IF ICOM <> 1 THEN RETURN
4240 IF B$ = CHR$(10) GOTO 4210
4250 IF B$ = CHR$(13) GOTO 4210
4260 RETURN
4270 '.....Subroutine to open the communication with the microprocessor
```

```
4280 CLOSE #2
4290 OPEN "COM2:9600,N,8,,CS100,DS100,CD100" FOR RANDOM AS #2
4300 RETURN
4310 '********************** DVM Instructions ***************************
4320 '..................... Open communications .........................
4330 'Open communication with external ADC: USER DEFINED !!!
4340 IF INTREAD = 1 THEN RETURN
4350 'ADDRESS = &H710                    'ADC Base Address
4360 'CHANNEL = 1                        'ADC Channel
4370 'OUT ADDRESS + 4, 128               'Initialize
4380 'OUT ADDRESS + 5, CHANNEL           'Select CHANNEL
4390 OPEN "COM1:9600,N,8,1,CS" FOR RANDOM AS #4'*
4400 'PRINT #4, "Z"'*
4410 FOR i = 1 TO 20000: NEXT i'*
4420 RETURN'*
4430 '*********************************************************************
4440 '......................... Data read ............................
4450 IF INTREAD = 1 THEN RETURN
4460 'External data read: USER DEFINED. Data must go to variable ZVALUE
4470 zvalue = 0!
4480 'FOR ADREAD = 0 TO 500
4490 '   OUT ADDRESS + 6, 0                      'Start a conversion
4500 '   IF INP(ADDRESS + 4) < 128 THEN 4170      'Wait for conversion
4510 '   LOW = INP(ADDRESS + 5)
4520 '   HIGH = INP(ADDRESS + 6)
4530 '   ZTEMP = 256 * HIGH + LOW
4540 '   IF ZTEMP > 32767 THEN ZTEMP = ZTEMP - 65536!
4550 '   ZVALUE = ZVALUE + ZTEMP / 204.8
4560 'NEXT ADREAD
4570 'ZVALUE = ZVALUE / ADREAD
4580 FOR i = 1 TO 27600: NEXT i
4590 PRINT #4, "Q1"'*
4600 INPUT #4, zvalue
4610 RETURN
4620 '*********************************************************************
4630 '*************************************************88
4640 'Graphing section of the program'*
4650 '*****************************************************
4660  choice$ = "full"'*
4670 INPUT "upper limit for vertical scale? ", highlock'*
4680 INPUT "lower limit for vertical scale? ", lowlock'*
```

```
4690 lowlim = -1 * npoints / 2'*
4700 uplim = npoints / 2'*
4710 CLS : WIDTH 80: SCREEN 9: COLOR 1, 3'*
4720 VIEW (70, 50)-(570, 300), 1, 15'*
4730 COLOR 12, 0: LOCATE 1, 30'*
4740 PRINT "graphics for Far-IR"'*
4750 COLOR 7, 0'*
4760 LOCATE 1, 6: PRINT "date"; DATE$'*
4770 LOCATE 1, 63: PRINT "time"; TIME$'*
4780 IF choice$ = "full" THEN'*
4790   COLOR 11, 0'*
4800   LOCATE 23, 8: PRINT lowlim'*
4810   LOCATE 23, 41: PRINT "0"'*
4820   COLOR 13, 0'*
4830   LOCATE 23, 50: PRINT "(step +ve)"'*
4840   LOCATE 23, 25: PRINT "(step -ve)"'*
4850   COLOR 11, 0'*
4860   LOCATE 23, 70: PRINT uplim'*
4870   LOCATE 4, 4: PRINT highlock'*
4880   LOCATE 22, 4: PRINT lowlock'*
4890   LOCATE 13, 8: PRINT lowlock + (highlock - lowlock) / 2!'*
4900   COLOR 13, 0'*
4910   LOCATE 8, 1: PRINT "lock+ve"'*
4920   LOCATE 18, 1: PRINT "lock-ve"'*
4930 END IF'*
4940 'these are for the little tick marks along the axis'*
4950 xmin = 0'*
4960 xmax = 500'*
4970 ymin = 0'*
4980 ymax = 225'*
4990 xinc = 50'*
5000 yinc = 25'*
5010 COLOR 11, 0'*
5020 xnumber = xmax - xmin'*
5030 ynumber = ymax - ymin'*
5040 xticks = (xnumber / xinc) + 1'*
5050 yticks = (ynumber / yinc) + 1'*
5060 xstart = 0'*
5070 ystart = 250'*
5080 ymin = 500 + ymin'*
5090 ymax = 500 - ymin'*
```

```
5100 xline = 18'*
5110 'now all the stuff is set up for the ticks'*
5120    LINE (250, 0)-(250, 275)'*
5130 ' 5  LINE (0, 125)-(500, 125)'*
5140 'now we want to make the axis so we can see what is going on'*
5150 FOR i = 1 TO xticks'*
5160     LINE (xstart, 245)-(xstart, 275)'*
5170     xstart = xstart + xinc'*
5180     xmin = xmin + xinc'*
5190     IF xmin > xmax THEN GOTO 5260'*
5200     FOR j = 1 TO yticks'*
5210         LINE (0, ystart)-(5, ystart)'*
5220         ystart = ystart - yinc'*
5230         IF ymin < ymax THEN GOTO 5260'*
5240     NEXT j'*
5250 NEXT i'*
5260  RETURN'*
5270 total = (-1 * npoints / 2 + istep) * 500! / npoints'*
5280 ifpoint = CINT(250 + total)'*
5290 icolor = 15'*
5300 rlock =300-((-1 * lowlock+interf(istep))/(highlock - lowlock) * 250)'*
5310   locker = CINT(rlock)'*
5320    IF istep = 1 THEN'*
5330     FOR x = ifpoint TO ifpoint: PSET (x, locker), icolor: NEXT x'*
5340    END IF'*
5350 '       IF istep > 1 THEN'*
5360 '        FOR x = ifpoint TO ifpoint: PSET (x, locker), icolor: NEXT '*
5370 '       END IF'*
5380    IF istep > 1 THEN LINE (xlast, fplast)-(ifpoint, locker), icolor'*
5390     xlast = ifpoint'*
5400     fplast = locker'*
5410 RETURN
5420 STOP
```

Appendix B

Two-Contact Resistance Probe

A two-contact resistance probe, shown in figure B.1, was constructed to check that the lead films were superconducting. A four foot brass tube with a diameter of approximately 1 cm was used. One end of the tube was partially cut away to provide a place to mount the sample. The sample holder was cut from a piece of insulating resin, and fixed into place with five minute epoxy. Two copper pads were attached to the outer edges of the resin insert with five minute epoxy, and two wires were fed through the tube to the copper pads. These wires were then soldered to the pads with Indium solder. At the other end of the tube, the copper wires were epoxied in place so that they would not fall into the tube, and also to prevent strain on the wires. The sample was placed onto the resin and glued down with epoxy. Fine copper wires were then silver-painted to the sample and soldered to copper pads. A plastic container was placed over the probe tip to protect the sample. A Fluke 75 multimeter was connected to the copper wires in order to monitor the resistance across the sample.

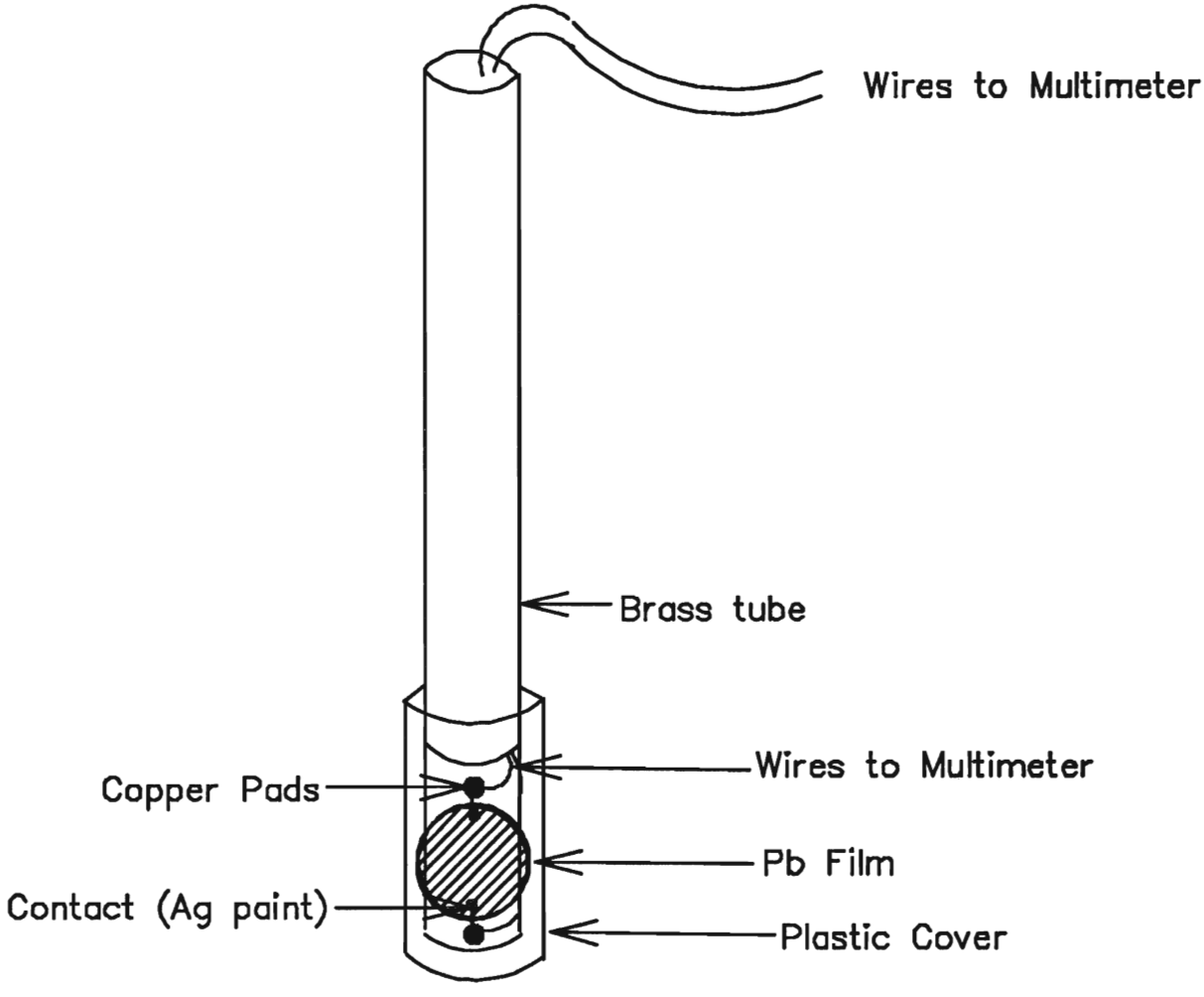

Figure B.1: Schematic of the layout of the resistance probe. Shown is the placement of the sample and the manner in which the electrical connections were made.

Bibliography

[1] B. Meyer *Low Temperature Spectroscopy* (American Elsevier Publishing Company, Inc., New York, 1971).

[2] K.D. Möller, W.G. Rothschild, *Far-Infrared Spectroscopy* (John Wiley & Sons, New York, 1971).

[3] D.H. Martin and E. Puplett, Infrared Physics, **10**, 105, 1969.

[4] M. Scholze, B.Sc. Thesis, Brock University, 1996.

[5] V.M. Da Costa and L.B. Coleman, Rev. Sci. Instrum., **61**, 2113, 1990.

[6] K. Yoshihara, A. Kitade, T. Matsushita, Jap. Journal of Appl Physics., **21**, L206, 1982.

[7] D.K. Lambert, P.L. Richards, Applied Optics, **17**, 1595, 1978.

[8] R.J. Bell, *Introductory Fourier Transform Spectroscopy* (Academic Press, New York, 1972).

[9] J. R. Meyer-Arendt, *Introduction to classical and modern Optics* (Englewood Cliffs, New Jersey, 1984).

[10] J.E. Stewart, *Infrared Spectroscopy* (Marcel Dekker, Inc., New York, 1970).

[11] Infrared Laboratories, *Instruction Manual for Model HDL-10 Dewar with Dual Helium-3 Refrigerators*, 1995.

[12] G. Chanin, J.P. Torre, ^{3}He Refrigerators and Bolometers for Infrared and Millimetre-Wave Observations, in *Infrared and Millimeter Waves, Vol. 10*, K.J. Button, editor (Academic press, Orlando, 1983).

[13] Oriel Corporation, *Optics Filters, Vol III*, (Oriel Corporation, Stratford, CT, 1990).

[14] *Handbook of Optical Constants of Solids, Vol. I and II*, E.D. Palik, editor, (Academic Press, San Diego, 1985).

[15] T. Kieliba, B.Sc. Thesis, Brock University, 1996.

[16] P.R. Griffiths, *Fourier Transform Infrared Spectrometry* (John Wiley & Sons, New York, 1986).

[17] J. Strong, G. A. Vanasse, Journal of the Optical Society of America, **49**, 844, 1959.

[18] E. Hecht, *Optics* (Addison-Wesley Publishing Company, Don Mills, Ontario, 1987).

[19] C. Kittel, *Introduction to Solid State Physics* (John Wiley & Sons, New York, 1986).

[20] F. Wooten, *Optical Properties of Solids* (Academic Press, Toronto, 1972).

[21] M. Born and E. Wolf, *Principles of Optics* (Pergamon Press, Oxford, 1975).

[22] Private communication with Dr. Reedyk.

[23] A. C. Rose-Innes and E. H. Rhoderick, *Introduction to Superconductivity* (Pergamon Press, Toronto, 1978).

[24] J. M Blatt, *Theory of Superconductivity* (Academic Press, New York, 1964).

[25] R. E. Glover and M. Tinkham, Physical Review, **108**, 243, 1957.

[26] D. C. Mattis and J. Bardeen, Physical Review, **111**, 412, 1958.

[27] E. H. Brandt, M. Bauer, E. Seider and L. Genzel, Proceedings of the USSR-FRG Bilateral Seminar, "Investigation of High Temperature Superconductors - Modern Spectroscopic and Microscopic Methods", Tallin, USSR, 1989.

[28] D. M. Ginsberg and M. Tinkham, Physical Review, **118**, 990, 1960.

[29] L. H. Palmer and M. Tinkham, Physical Review, **165**, 588, 1968.

[30] For a summary see S. Perkowitz, Submillimeter Solid-State Physics, in *Infrared and Millimeter Waves, Vol. 8*, K. J. Button, editor, (Academic Press, Toronto, 1983).

[31] *Handbook of Chemistry and Physics*, R. C. Weast, ed. (The Chemical Rubber Co., Cleveland, 1969).

[32] The Random House College Dictionary, revised edition, L. Urdang, editor, (Random House, Inc., 1988).

[33] A. Lehninger, D. Nelson and M. Cox, *Principles of Biochemistry* (Worth Publishers, New York, 1993).

[34] Private communication with Dr. Pink.

[35] U. Buontempo, G. Careri, Biopolymers, **10**, 2377, 1971.

[36] W. J. Shotts, A. J. Sievers, Biopolymers, **13**, 2593, 1974.

[37] H. Fröhlich, Proc. Nat. Acad. Sci. USA, **72**, 4211, 1975.

[38] K. D. Moller, G. P. Williams, S. Steinhauser, C. Hirschmug, J. C. Smith, Biophysical Journal, **61**, 276, 1992.

[39] V. Buontempo, G. Careri, P. Fasella, Physics Letters, **31A**, 543, 1970.

[40] Y. N. Chirgadze, A. M. Ovsepyan, Biopolymers, **12**, 637, 1973.

[41] G. J. Evans, M. W. Evans, Spectrochimica Acta, **38A**, 421, 1982.

[42] M. Ataka, S. Tanaka, Biopolymers, **18**, 507, 1979.

[43] Sciencetech Inc. *Sciencetech Instruction Manual for SPS-200 Polarizing Roofmirror Interferometer*, 1995.